

# Development and Recent Progress on Ammonia Synthesis Catalysts for Haber–Bosch Process

John Humphreys, Rong Lan, and Shanwen Tao\*

Due to its essential use as a fertilizer, ammonia synthesis from nitrogen and hydrogen is considered to be one of the most important chemical processes of the last 100 years. Since then, an enormous amount of work has been undertaken to investigate and develop effective catalysts for this process. Although the catalytic synthesis of ammonia has been extensively studied in the last century, many new catalysts are still currently being developed to reduce the operating temperature and pressure of the process and to improve the conversion of reactants to ammonia. New catalysts for the Haber–Bosch process are the key to achieving green ammonia production in the foreseeable future. Herein, the history of ammonia synthesis catalyst development is briefly described as well as recent progress in catalyst development with the aim of building an overview of the current state of ammonia synthesis catalysts for the Haber–Bosch process. The new emerging ammonia synthesis catalysts, including electride, hydride, amide, perovskite oxide hydride/oxynitride hydride, nitride, and oxide promoted metals such as Fe, Co, and Ni, are promising alternatives to the conventional fused-Fe and promoted-Ru catalysts for existing ammonia synthesis plants and future distributed green ammonia synthesis based on the Haber–Bosch process.

method for ammonia synthesis from H<sub>2</sub> and N<sub>2</sub> under high pressure and temperature using recycling.<sup>[2]</sup> This process was industrialized by Carl Bosch, with the first ammonia synthesis plant being built in 1911.<sup>[2]</sup> Due to this the process of producing ammonia from H<sub>2</sub> and N<sub>2</sub> at high temperature and pressure is known as the Haber–Bosch process.<sup>[2]</sup> Fritz Haber and Carl Bosch won the Nobel Prize in Chemistry in 1918 and 1931 respectively for their work on this process. In 2007, Gerhard Ertl won the Nobel Prize in Chemistry for his great contribution on the surface chemistry of iron catalysts.<sup>[3]</sup> Today most ammonia synthesis plants use fused-iron catalysts that use a variety of carefully designed promoter materials. As will become evident, these plants require high pressure and temperature to achieve the desired conversion and as such require a significant energy input. It is therefore the goal of any new ammonia synthesis catalyst to ease these conditions

## 1. Introduction


The production of ammonia over the last century has been fundamental in supporting the increase in population due to its use as a fertilizer. The use of ammonia in fertilizers, which provide a fixed nitrogen source, has supported ≈27% of the world's population over the last century.<sup>[1]</sup> To facilitate the massive increase in demand, German chemist Fritz Haber in 1908 developed a

by achieving high catalytic activity at reduced temperatures and pressures, enabling a more energy-efficient process.

In the conventional Haber–Bosch process, fossil fuels such as natural gas and coal are normally used as the energy sources for ammonia synthesis, releasing millions of tonnes of CO<sub>2</sub> to the atmosphere, which is about 1–2% of the global CO<sub>2</sub> emission.<sup>[1,4,5]</sup> The use of low-carbon renewable energy sources has been proposed to produce green ammonia. According to the roadmap for ammonia economy, in the foreseeable future, the Haber–Bosch process is still the dominant ammonia synthesis technology, although other emerging technologies such as electrochemical and photocatalytic synthesis of ammonia are also promising.<sup>[5–7]</sup> Green ammonia production can alleviate the pressure on renewable electricity storage if the “surplus” electricity from wind and solar energy is used as the energy source for ammonia synthesis.<sup>[4]</sup> New robust catalysts for agile operation of small-scale distributed green ammonia synthesis are in demand. As renewable energy technologies advancing the possibility of running green ammonia production through the Haber–Bosch process increase, H<sub>2</sub> production from electrolyzers powered through renewable energy offers a more energy-efficient alternative to the conventional methane-reforming process while lowering carbon emissions. In a review recently published by Smith et al., they calculated that an ammonia loop fed with H<sub>2</sub> from an electrolyzer would produce 0.38–0.53 tonnes of CO<sub>2</sub> per tonne of NH<sub>3</sub> compared to 1.673 tonnes of CO<sub>2</sub> per

Dr. J. Humphreys, Dr. R. Lan, Prof. S. Tao  
School of Engineering  
University of Warwick  
Coventry CV4 7AL, UK  
E-mail: S.Tao.1@warwick.ac.uk

Prof. S. Tao  
Department of Chemical Engineering  
Monash University  
Clayton, Victoria 3800, Australia

 The ORCID identification number(s) for the author(s) of this article can be found under <https://doi.org/10.1002/aesr.202000043>.

© 2020 The Authors. Advanced Energy and Sustainability Research published by Wiley-VCH GmbH. This is an open access article under the terms of the Creative Commons Attribution License, which permits use, distribution and reproduction in any medium, provided the original work is properly cited.

DOI: 10.1002/aesr.202000043

tonne of NH<sub>3</sub> for the loop with H<sub>2</sub> from methane reforming.<sup>[8]</sup> The electrolyzer loop would also improve energy efficiency by 50%.<sup>[8]</sup> In their calculations they used an electrolyzer efficiency of 60% in line with those currently available. However, future research into more efficient electrolyzers will further increase the viability of this process. Through redesigns of the ammonia synthesis loop involving the replacement of the condenser with absorption of ammonia, the potential for highly active novel ammonia catalysts greatly increases. Catalysts that can tolerate and facilitate quick start-up and agile operation will be key to dealing with the intermittent nature of renewable energy. As such, catalysts with high activity at low operating conditions (pressure and temperature) that have good impurity tolerance for agile operation of plants go hand in hand with green ammonia production. From this point of view, the search for better catalysts for efficient synthesis of ammonia through the Haber–Bosch process is key for achieving green ammonia.

The reaction of hydrogen and nitrogen to produce ammonia is as follows<sup>[2,9]</sup>



From this it can be seen that the reaction is exothermic with a high pressure and low temperature favoring ammonia synthesis at equilibrium conditions. Although the theoretical ammonia equilibrium concentration can be close to 100% at low temperatures and high pressures, the ammonia formation rate is extremely slow and not suitable for production purposes.<sup>[2]</sup> Due to this the Haber–Bosch process is conducted at high temperature and pressure. However, at these conditions the equilibrium shifts so as to decompose the produced ammonia and give a lower production rate.

The catalytic synthesis of ammonia relies on the surface reaction of nitrogen and hydrogen on the catalyst surface. This surface reaction is achieved through the chemisorptions of the reactants on to the catalyst surface.<sup>[2]</sup> This differs from the other adsorption process of physisorption due to the formation of a chemical bond with surface and reactants.<sup>[10]</sup> How the reactants behave when in the adsorption phase is the essence of catalyst theory. Liu published a book and a comprehensive review of catalytic ammonia synthesis, mainly on the principles and theory of ammonia synthesis.<sup>[2,3]</sup> Jennings also edited a book on catalytic ammonia synthesis fundamentals and practice.<sup>[11]</sup> Recently, Saadatjou et al. have published a review on the use of ruthenium catalysts for ammonia synthesis from nitrogen and hydrogen.<sup>[12]</sup> The focus of this review will be on the catalytic activity of iron, cobalt, nickel, and nitride catalyst systems plus the latest progress on electride, hydride, nitride, oxynitride hydride promoted Ru, Fe, Co, and Ni catalysts for ammonia synthesis. The basic structure of this review is highlighted in **Figure 1**. These catalysts can be used for both conventional centralized large-scale Haber–Bosch ammonia synthesis plants and distributed small-scale green ammonia production via the same process.

## 2. Principles of Catalyst Mechanism

The proposed reaction mechanisms for the catalyzed reaction of nitrogen and hydrogen to form ammonia are as follows<sup>[13]</sup>

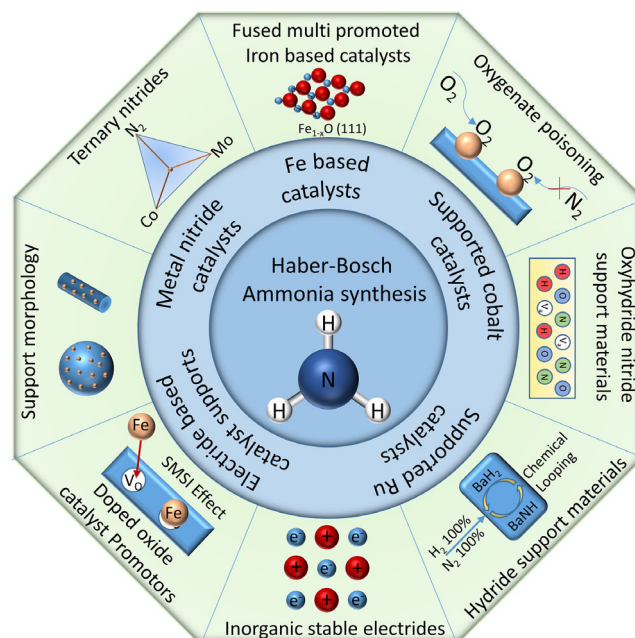
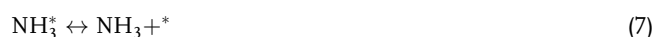


**Figure 1.** Graphical overview of strategies to improve Haber–Bosch ammonia synthesis.



This reaction model was proposed by Stolze and Norskov.<sup>[14]</sup> AQ second model was proposed by Bowker,<sup>[15]</sup> which has the dissociative adsorption of hydrogen take place in two steps instead of one. From this model there are three proposed rate-limiting steps, which are 1) the dissociative adsorption of dinitrogen,<sup>[16]</sup> 2) the reaction on the catalyst surface of adsorbed species,<sup>[17]</sup> and 3) the desorption of ammonia.<sup>[18]</sup>

However, after extensive surface science experiments it is generally accepted that the dissociative adsorption of N<sub>2</sub> is the rate-limiting step.<sup>[19]</sup> As early as 1934, P.H. Emmett and S. Brunauer<sup>[20]</sup> examined the adsorption of N<sub>2</sub> on the iron ammonia synthesis catalyst over a range of temperatures (273–450 °C) and pressures (0.1–50 MPa), finding that the rate of nitrogen adsorption was in the correct order of magnitude to be the rate-determining step for ammonia synthesis.<sup>[20]</sup> Extensive research on nitrogen interaction on the iron surface was conducted by Ertl et al.<sup>[21–24]</sup> Using techniques such as Auger electron spectroscopy, UV photoelectron spectroscopy, thermal desorption spectroscopy, work function measurements, and low-energy electron diffraction, they investigated the adsorption

of nitrogen on iron single-crystal surfaces for both Fe(100) and Fe(111) over a temperature range 140–1000 K to come to the conclusion that nitrogen adsorption is the rate-limiting step in the ammonia synthesis reaction.<sup>[24]</sup> Even after many experiments involving the adsorption of N<sub>2</sub>, there is still controversy over the exact mechanism of this step. It is unknown whether the N<sub>2</sub> dissociates directly to nitrogen atoms on the catalyst surface or whether this dissociation to nitrogen atoms takes place on intermediates. This has been experimentally tested in numerous experiments but different conclusions were reached for a variety of different metals and crystal faces and at different conditions.<sup>[25,26]</sup> This is most notable at conditions used in industrial synthesis, where high pressures are involved. Spencer<sup>[18]</sup> provides a detailed breakdown of the rate-determining step for the ammonia synthesis reaction with the conclusion that the concept of a single step to determine the rate is too simple, especially in industrial conditions. This is supported by work conducted by Johnson and Roberts,<sup>[27]</sup> in which nitrogen was easily dissociated on an iron surface at 80 K. In their work Ertl et al.<sup>[17]</sup> found that the highest activation energy of the reaction steps was for the reaction on the catalyst surface of adsorbed species with a value of 117 kJ mol<sup>-1</sup> compared to 42 kJ mol<sup>-1</sup> for nitrogen dissociation.

The thermodynamic equilibrium of the ammonia synthesis process is important to understand to evaluate the potential maximum ammonia yield of a catalyst at certain conditions. In 1906 Fritz Haber calculated the equilibrium yield of ammonia from nitrogen and hydrogen at temperatures from 200 to 1000 °C under pressures of 1, 30, 100, and 200 atm.<sup>[28]</sup> The thermodynamic equilibrium data published by Max Appl<sup>[29]</sup> calculated from Gillespie and Beatties's<sup>[30]</sup> work has been reproduced in **Figure 2**.

From this we can determine under what conditions the highest theoretical ammonia yield can be achieved. Therefore, the goal of any catalyst for ammonia synthesis should be to reach its maximum yield at low temperature to achieve a higher yield due to the limit imposed by thermodynamic equilibrium. As mentioned earlier the reaction rate at low temperatures is too

slow to feasibly produce ammonia despite the large equilibrium limit, which almost reaches 100% conversion. Most modern ammonia synthesis catalysts used in the Haber–Bosch process are reported to achieve a conversion rate of around 10–15% operating in the range of 425–450 °C at pressures above 100 atm.<sup>[2]</sup> From this it can be seen that if catalysts can be developed to increase the rate of reaction at temperatures lower than this then the conversion per pass of the ammonia synthesis loop will increase exponentially. For this reason, the catalytic activity of the catalyst is of key importance. If the activity of new catalysts is high enough, ammonia synthesis can be achieved at reduced temperature and pressure, which is anticipated to have a higher overall energy efficiency. The activities of key ammonia synthesis catalysts are summarized below.

The catalysts used in the process discussed previously generally fall into one of two categories, fused-iron and supported metallic catalysts. Fused-iron catalysts are the most widely applied of all the ammonia synthesis catalysts.<sup>[2,31–46]</sup> These catalysts are derived from iron oxides, of which there are three possibilities: Fe<sub>2</sub>O<sub>3</sub>, Fe<sub>3</sub>O<sub>4</sub>, and Fe<sub>1-x</sub>O,<sup>[2,10]</sup> which are known as hematite, magnetite, and wüstite, respectively. Hematite has a rhombohedral crystal lattice structure with the unit cell containing four Fe<sup>3+</sup> ions and six O<sup>2-</sup> ions.<sup>[10]</sup> Magnetite has the spinel-type cubic crystal lattice structure with a unit cell containing eight Fe<sub>3</sub>O<sub>4</sub> molecules; it is this iron oxide that has been the basis of ammonia synthesis catalysts over the last century.<sup>[10]</sup> Wüstite has a NaCl-type cubic lattice structure with each unit cell containing four FeO molecules.<sup>[10]</sup> Although magnetite makes up the majority of industrial ammonia synthesis catalysts, wüstite has gained considerable interest with the highest reported activities of the three.<sup>[2]</sup> Industrially, these iron catalysts will be multipromoted with promoters such as K<sub>2</sub>O, BaO, and Al<sub>2</sub>O<sub>3</sub> are present in small quantities of a few weight percentage.<sup>[47]</sup> These provide the catalysts with a range of structural and electronic promotion that will be examined more closely in the following review of the literature.

Supported metallic catalysts are catalysts made up of a metallic catalyst material, normally ruthenium or cobalt for the ammonia synthesis reaction, present on the surface of a support material, normally activated carbon or a metal oxide.<sup>[2]</sup> Commonly the weight percentage of the metallic catalyst is around 2–10%. Supporting these metallic catalyst materials is done for the following reasons. First, when compared to iron the cost of ruthenium and cobalt is significantly higher; therefore, by using a support material to make up the bulk of the catalyst the cost can be brought in line with that of the iron catalyst. Second, by tailoring the support material to the specific catalyst, promotion effects can be achieved, greatly altering the catalyst activity.

The design of the ammonia synthesis loop is an in-depth topic that has been covered extensively elsewhere.<sup>[2,29,48,49]</sup> However, it is important to highlight the key concepts of this process to understand the goals of ammonia synthesis catalyst development and how the said catalysts can be implemented. In the simplest terms, the ammonia synthesis loop consists of an ammonia converter, which catalytically converts the synthesis gas to ammonia; a compressor, which is used to achieve the desired pressure for the synthesis gas and to recycle the stream before it enters the converter; and a condenser, which can be located either after or before (but after the recycle stream has been combined with

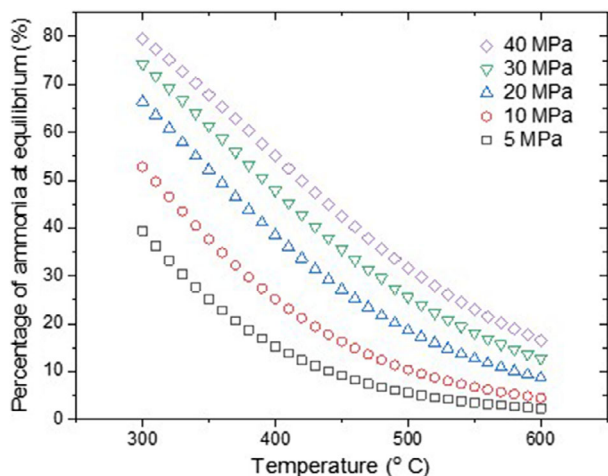


**Figure 2.** Effect of temperature and pressure on the percentage of ammonia at equilibrium reproduced from Max Appl “Ammonia, 2. Production processes”.<sup>[29]</sup>

the synthesis gas) the convertor to separate the produced ammonia.<sup>[29]</sup> This design imparts some key considerations on ammonia catalyst development. Running the synthesis loop at reduced pressure may appear appealing as this will not only lower the duty of the compressor but allow for savings on construction materials as lower-pressure-rated designs can be used. However, as ammonia is removed from the system through a condenser, it follows that, as the synthesis loop pressure is decreased, the refrigerator power will have to be increased to achieve the lower temperatures required for separation. This can be quantified in practical terms through examining both the Kellogg advanced ammonia process (KAAP) and Topsøe processes, which use synthesis loop pressures of 9.1 and around 25 MPa, respectively.<sup>[2]</sup> At 9.1 MPa the Kellogg advanced ammonia process requires a condenser temperature of  $-20^{\circ}\text{C}$ , whereas the Topsøe processes normally use condenser temperatures of between  $0$  and  $-10^{\circ}\text{C}$ .<sup>[2]</sup> The effect of pressure on the synthesis loop efficiency was calculated by Liu for an iron-based catalyst (ZA-5) producing 330 tonnes of ammonia per day at both 10 and 30 MPa.<sup>[2]</sup> At 10 MPa the efficiency of circulation compression and refrigeration was worse, with a circulation compressor duty of 295 kW and a refrigeration compressor duty of 311 kW compared to 240 and 184 kW, respectively, for 30 MPa. However, the duty of the fresh syngas compressor rises from 7970 to 10 410 kW as the pressure goes from 10 to 30 MPa, significantly offsetting the increase in refrigeration and circulation compressor duty.<sup>[2]</sup> To further add to this, it should be noted that the catalyst volume is nearly four times as large in the 10 MPa loop to achieve the required conversion per pass. As such it is evident that a balancing act must be achieved when aiming to lower the ammonia synthesis loop pressure, although real benefits can be achieved by aiming for synthesis loops operating at just under 10 MPa. It has been suggested that the condensation step of the ammonia synthesis loop could be preplaced by absorption of ammonia in crystalline salts, which can absorb ammonia at partial pressures as low as 0.002 bar at moderate temperatures.<sup>[50–53]</sup> The implementation of this over the conventional condenser for separation has the potential to allow ammonia synthesis loops to operate at pressures as low as 30 bar.<sup>[8]</sup> From the thermodynamic data shown earlier, the benefits of operating at lower temperature can be seen. At lower temperatures the theoretical maximum conversion to ammonia is increased. However, as the ammonia synthesis reaction is exothermic, running the convertor at lower temperatures requires better heat removal from the convertor. Numerous different convertors have been designed over the years; however, most of these can be divided into two categories: tube-cooled convertors and quench convertors.<sup>[29]</sup> Tube-cooled convertors are internally cooled through tubes in the catalyst bed, the cooling medium normally being the reactor feed gases to reach the reaction temperature. Quench convertors use multiple catalyst beds that operate adiabatically with part of the reactor feed gas used as the quench between beds. Therefore, implementation of new catalysts that show improved activity at lower pressures and temperatures must be done with great care. Despite this it can be seen that significant reductions in operating pressure can be achieved while maintaining viable condenser temperatures, while the significant increases in conversion at lower temperature can outweigh the demand on convertor heat removal. As such the

current goal of researchers in the field of ammonia synthesis catalysts is to develop catalysts that exhibit increased activity at lower temperatures, with activities suitable for ammonia synthesis at loop pressures of around 10 MPa.

### 3. Iron Catalysts

#### 3.1. Early Development of Iron-Based Catalysts

Fused-iron catalysts are by far the most studied and widely applied of all the ammonia synthesis catalysts.<sup>[2,31–46]</sup> As mentioned in the previous section, fused-iron catalysts are derived from three possible iron oxides,  $\text{Fe}_2\text{O}_3$  (hematite),  $\text{Fe}_3\text{O}_4$  (magnetite), and  $\text{Fe}_{1-x}\text{O}$  (wüstite). Of these, catalysts derived from  $\text{Fe}_3\text{O}_4$  are the most commonly used in industrial ammonia synthesis.

The crystal structures of iron oxides from perspective side views is shown in **Figure 3**.

The first ammonia synthesis catalysts were based on magnetite with the commonly held belief that this structure provided the best activity for ammonia synthesis. Therefore, the majority of catalyst development over the last century was devoted to the promoters of the magnetite catalysts that were used to increase catalytic activity. Magnetite is ferromagnetic with the inverse spinel crystal structure.<sup>[10,54]</sup> The  $\text{Fe}^{2+}$  and  $\text{Fe}^{3+}$  ions are located in the interstitial sites with the O anions forming a close-packed fcc sublattice.<sup>[10]</sup> To determine the optimal ratio of  $\text{Fe}^{2+}$  to  $\text{Fe}^{3+}$  ions, Almquist and Crittenden<sup>[55]</sup> conducted studies to show how the catalytic activity varies with this ratio in magnetite, and they found that a value close to 0.5 was optimal. This work was continued by Bridger et al.<sup>[56]</sup> using promoters of  $\text{Al}_2\text{O}_3\text{--K}_2\text{O}$ . In their results they obtained a volcano-type plot showing how the conversion percentage varied with the  $\text{Fe}^{2+}/\text{Fe}^{3+}$  ion ratio, which agreed with the conclusion of Almquist and Crittenden<sup>[55]</sup> that the optimal  $\text{Fe}^{2+}/\text{Fe}^{3+}$  ion ratio is 0.5.

#### 3.2. Promoted Fe-Based Catalysts

Although iron makes up the basis of most industrial ammonia synthesis catalysts, it shows no activity on its own at the conditions required. Therefore, it is necessary to promote these catalysts with a range of promoter materials that provide both structural and electronic promotion effects.

In 1970 Aika and Ozaki<sup>[57]</sup> investigated the use of an  $\text{Al}_2\text{O}_3$  promoter with an iron catalyst using 2.2 wt% of the promoter. Although no yield increase was noted over their test of the unpromoted catalyst,<sup>[58]</sup> they confirmed the use of  $\text{Al}_2\text{O}_3$  as a sintering preventer. In 1972, Baranski et al.<sup>[59]</sup> investigated the kinetics of reduction for iron catalysts used for ammonia synthesis, finding a link between the gas flow rate, temperature, and reduction degree. Small iron particles were investigated for their structural sensitivity toward ammonia synthesis by Dumesic et al. in 1975.<sup>[60]</sup> Van Ommen et al. studied the potassium promoter in a number of studies.<sup>[61,62]</sup> The first experiments promoted with KOH resulted in a reduction in activity due to the potassium remaining in the hydroxide form under the synthesis conditions and producing a strong interaction with the iron surface.<sup>[61]</sup> Further experiments revealed that potassium promoters

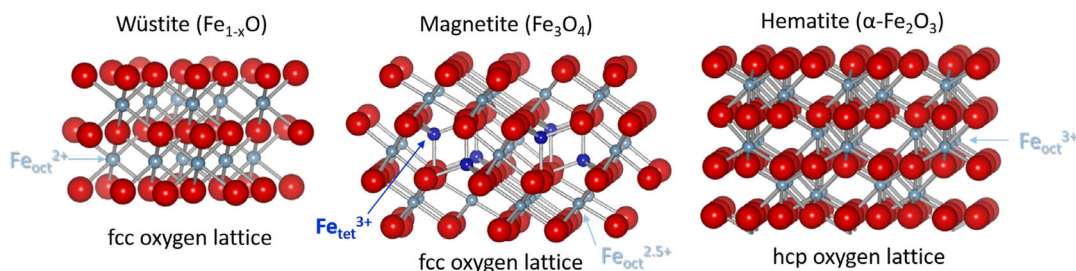


**Figure 3.** Perspective side views of Fe-oxide crystal structures. Reproduced with permission.<sup>[152]</sup> Copyright 2016, Elsevier.

performed poorly at low pressure but when the pressure was increased much higher activities could be unlocked.<sup>[62]</sup> This was confirmed by other work in the potassium promoter.<sup>[63,64]</sup> In addition to the pure iron-based catalysts, iron alloys were also investigated as ammonia synthesis catalysts. The investigation of iron alloy catalysts was studied in 1982 by Taylor et al.<sup>[65,66]</sup> Their work involved both iron-cobalt and iron-nickel catalysts, with both showing improved activity over the pure iron catalyst. However, nickel is much more expensive than iron, which could be the major reason that this kind of catalyst has not been commercialized. Low-iron-content catalysts using  $\gamma$ -Al<sub>2</sub>O<sub>3</sub> as the support were investigated by Homs et al. in 1984.<sup>[67]</sup> As expected, the low iron content resulted in much lower activity than that of other reported catalysts at the time but did provide insight into the nature of promotion with an increase in activity as the H<sup>+</sup> concentration increased. This did have a limit of 8 mmol g<sup>-1</sup> H<sup>+</sup> in the  $\gamma$ -Al<sub>2</sub>O<sub>3</sub> support, after which the activity decreased. Bare et al.<sup>[68]</sup> reported alumina and potassium promoters on an iron single crystal showing that these promoters provide no electronic promotion. This work was continued by Strongin et al.<sup>[69]</sup> Similar to the iron-cobalt and iron-nickel alloys, Baiker et al. investigated an Fe<sub>91</sub>Zr<sub>9</sub> catalyst in 1987<sup>[70–72]</sup> showing good activity.

The activity of Fe-based catalysts is related to the face of the iron crystals. In 1982, Spencer et al. investigated the effects of the surface structure for single-crystal iron catalysts for ammonia synthesis.<sup>[73]</sup> The planes studied were the close-packed (110) plane with six coordinated atoms exposed, the (100) plane, which has four coordinated atoms exposed and is less closely packed, and the (111) plane, which has the most open surface and contains four coordinated and seven coordinated atoms exposed. It was found that the (111) crystal surface had the highest ammonia synthesis rate by an order of magnitude compared to (100) and (110). Further work into the face of the iron crystal was reported by Strongin et al.<sup>[74]</sup> in 1987, in which the seven coordinated sites (C<sub>7</sub>) were further confirmed to be the major factor dictating the activity of the crystal face toward ammonia synthesis. Again, the (111) plane was shown to be the most active, with good activity also shown for (211). The low activity for (210) confirmed that surface roughness was not an import factor for crystal face activity, further emphasizing the importance of C<sub>7</sub> sites. Their ordering of plane activity was as follows: (111) > (211) > (100) > (210) > (110).<sup>[74]</sup>

In 2015, Han et al. prepared a Nb<sub>2</sub>O<sub>5</sub>-promoted wüstite-based catalyst for ammonia synthesis.<sup>[75]</sup> To produce this catalyst appropriate amounts of magnetite, iron, alumina, potassium nitrate,

calcium carbonate, and other promoters were melted with 0.6 wt% Nb<sub>2</sub>O<sub>5</sub> at 1600 °C before crushing and sieving to obtain a catalyst with a granule size range of 1.0–2.0 mm.<sup>[75]</sup> Although the results suggest that the catalyst with Nb<sub>2</sub>O<sub>5</sub> has a slightly lower activity than the catalyst prepared without Nb<sub>2</sub>O<sub>5</sub> (around 19% ammonia outlet concentration compared to 18% outlet concentration for the Nb<sub>2</sub>O<sub>5</sub>-promoted catalyst at 450 °C, 30 000 h<sup>-1</sup>, and 15 MPa), it was shown by TG experiments that it had a reduction temperature around 25 °C lower than that of the non-Nb<sub>2</sub>O<sub>5</sub>-promoted catalyst, avoiding difficulties faced by sintering of the nonpromoted catalyst.<sup>[75]</sup> It also achieved the reduction at a much faster rate, which would improve commissioning times in ammonia synthesis plants. The activities of reported typical iron-based catalysts are listed in **Table 1**. Comparing the results is challenging because the operating conditions are quite different. Generally, the Al<sub>2</sub>O<sub>3</sub>, K<sub>2</sub>O, CaO, and SiO<sub>2</sub>-promoted iron catalysts exhibit high activity with an ammonia conversion of 15–20% at the converter outlet achieved for space velocities of 30 000–10 000 h<sup>-1</sup> at 425 °C and 150 bar.<sup>[47]</sup>

Recent results reported by Wang et al.<sup>[76]</sup> have shown the excellent promotion effect lithium hydride has on the activity of iron along with metal hydrides toward ammonia synthesis when present in a 5 to 1 molar ratio to iron. Unlike the established norm as seen in the other reported catalysts thus far in which the bulk of the catalyst is iron with promoters present in a small weight percentage, this low-iron-content catalyst provides significant activity at temperatures substantially lower than those previously seen. The iron content is only  $\approx$ 58% in this catalyst, which opens up a previously underinvestigated area of catalyst development of iron catalysts with reduced iron content. However, the practical application of these hydride catalysts might be limited by the sophisticated preparation process and by their high sensitivity to air and moisture.<sup>[77,78]</sup>

Hydride catalysts were further investigated with iron as reported by Gao et al.<sup>[79]</sup> Good activity was achieved at low temperatures for low iron content with a 20% Fe–BaH<sub>2</sub> catalyst. However, the major impact of their results comes from the implementation of the chemical looping process for ammonia synthesis. In this process pure nitrogen feeds and pure hydrogen feeds are alternated to create a loop of synthesis gas as compare to the conventional process in which hydrogen and nitrogen are fed together in a 3 to 1 ratio. In the chemical looping process, nitridation of the hydride support occurs under the pure nitrogen flow, followed by the formation of ammonia through the hydrogenation of the nitridated hydride. When this process was used,

**Table 1.** Chemical composition and activity of selected iron catalysts for ammonia synthesis.

Catalyst	Promoter [wt%]	Reactor temperature [°C]	Reactor pressure [MPa]	Weight hourly space velocity (WHSV) [mL g <sup>-1</sup> h <sup>-1</sup> ]	NH <sub>3</sub> percentage in reactor outlet [v/v%]	NH <sub>3</sub> synthesis rate [μmol g <sup>-1</sup> h <sup>-1</sup> ]	Ref.
7% Fe/CeO <sub>2</sub> (applied electric field 6 mA)	–	100	0.1	144 000	–	155	[83]
20% Fe–BaH <sub>2</sub> (chemical looping synthesis)	–	300	0.1	60 000	–	1703	[79]
2.8% Fe/γ-Al <sub>2</sub> O <sub>3</sub>	–	320	0.1	–	–	0.12	[67]
20% Fe–BaH <sub>2</sub>	–	350	0.1	60 000	–	384	[79]
Fe(95%)Co(5%)	–	400	0.1	–	–	820.07	[65]
Fe(85%)Ni(15%)	–	400	0.1	–	–	334.354	[65]
1.2% Fe/BaCeO <sub>3-x</sub> H <sub>y</sub> N <sub>z</sub>	–	400	0.9	36 000	–	6800	[82]
Fe <sub>91</sub> Zr <sub>9</sub>	–	417	0.9	–	–	72	[70]
Fe–5LiH	–	300	1	60 000	–	4840	[153]
Fe/LiH	40%LiH	350	1	60 000	–	11 428	[76]
10% Fe/C	3.5%Ba	400	1	53 400	–	14 400	[154]
80% Fe/Ce <sub>0.8</sub> Sm <sub>0.2</sub> O <sub>2-δ</sub>	–	450	1	16 000	–	8700	[84]
Fe <sub>1-x</sub> O	–	400	3	–	7.94	–	[2]
FePc	10% Cs	400	3	12 000	–	14 000	[155]
Fe-Metal organic framework derived catalyst (MDC)	1% K	400	3	13 500	–	30 400	[156]
Fe <sub>1-x</sub> O	(Al <sub>2</sub> O <sub>3</sub> + CaCO <sub>3</sub> + K <sub>2</sub> CO <sub>3</sub> ) <10 wt%	430	3	7200	–	11 900	[157]
Fe <sub>3</sub> O <sub>4</sub>	(Al <sub>2</sub> O <sub>3</sub> + CaCO <sub>3</sub> + K <sub>2</sub> CO <sub>3</sub> ) <10 wt%	430	3	7200	–	9200	[157]
1% Fe/BaTiO <sub>3-x</sub> H <sub>x</sub>	–	400	5	66 000	–	14 000	[81]
10% Fe/C	K	470	9	140 000	4.58	–	[158]
2% Co–8% Fe/C	K	470	9	140 000	6.04	–	[158]
FeOOH/Al <sub>2</sub> O <sub>3</sub>	K (5 wt%)	500	9	26 400	–	32 850	[159]
Fe <sub>1-x</sub> O	–	425	10	–	19.23	–	[2]
ZBRW-10 (wustite)	Al <sub>2</sub> O <sub>3</sub> (2.18 wt%) + CaO (1.3 wt%) + K <sub>2</sub> O (0.44 wt%) + CoO (2.1 wt%)	450	10	–	10.8	–	[160]
Fe <sub>3</sub> O <sub>4</sub>	2.4% Al <sub>2</sub> O <sub>3</sub> , 1.4% CaO, 0.6% K <sub>2</sub> O, 0.34% SiO <sub>2</sub> , 0.3% MgO	425	15	–	20.8	–	[47]
Fe <sub>3</sub> O <sub>4</sub>	2.3% Al <sub>2</sub> O <sub>3</sub> , 1.1% CaO, 0.58% K <sub>2</sub> O, 0.33% SiO <sub>2</sub> , 0.3% MgO	425	15	–	21.0	–	[47]
Fe <sub>3</sub> O <sub>4</sub>	2.4% Al <sub>2</sub> O <sub>3</sub> , 1.1% CaO, 0.58% K <sub>2</sub> O, 0.39% SiO <sub>2</sub> , 0.4% MgO, 0.5% Co <sub>3</sub> O <sub>4</sub>	425	15	–	21.1	–	[47]
Fe <sub>3</sub> O <sub>4</sub>	Al <sub>2</sub> O <sub>3</sub> , K, Ca, 0.6% Nb <sub>2</sub> O <sub>5</sub>	450	15	–	18	–	[75]

the activity of the 20% Fe–BaH<sub>2</sub> catalyst increased by ≈4.5 times at a temperature 50 °C lower.<sup>[79]</sup> Interestingly, when iron was replaced with nickel in this catalyst, a drastic increase in activity was observed. Nickel is known to show some activity toward ammonia synthesis,<sup>[80]</sup> but its results have never been high enough to compete with the leading Fe catalysts. However, when the 20% Ni–BaH<sub>2</sub> catalyst was used in the chemical looping process, it achieved an activity higher than the 20% Fe–BaH<sub>2</sub> catalyst and an activity 40 times higher than the same nickel catalyst used in the conventional catalytic process. The activity of this 20% Ni–BaH<sub>2</sub> catalyst in the chemical looping process at 300 °C and 0.1 MPa is 2033 μmol g<sup>-1</sup> h<sup>-1</sup>.<sup>[79]</sup> Further details on these catalysts have been laid out in a review article recently published by Gao et al.<sup>[78]</sup>

Low-iron-content catalysts were taken even further in a study by Tang et al.,<sup>[81]</sup> in which iron was supported on the oxyhydride material BaTiO<sub>3-x</sub>H<sub>x</sub>, with an iron weight percentage of 1 wt%. The activity of this catalyst was 14 mmol g<sup>-1</sup> h<sup>-1</sup> and was achieved at 400 °C and 5 MPa, with the high activity relative to iron content expected to be caused by an increased resistance to hydrogen poisoning as well as the electron promotion effect of the oxyhydride support.<sup>[81]</sup> Further low-iron-content experiments were conducted by Kitano et al.<sup>[82]</sup> in which nitrogen was incorporated into an oxyhydride material. The oxynitride-hydride used was BaCeO<sub>3-x</sub>H<sub>y</sub>N<sub>z</sub> with iron supported in a quantity of 1.2 wt%. Again, high activity when compared to the low iron content was obtained, 6.8 mmol g<sup>-1</sup> h<sup>-1</sup> at 400 °C and 0.9 MPa. When using this catalyst, they found that the rate-limiting step was no longer

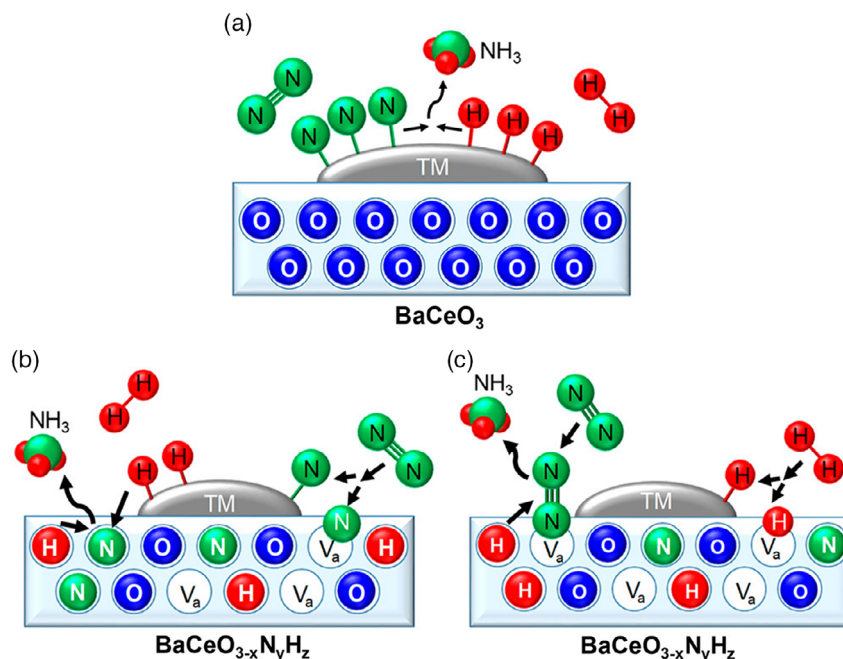


**Figure 4.** a) Conventional mechanism for ammonia synthesis on a transition metal catalyst supported on  $\text{BaCeO}_3$ . b,c) Proposed mechanisms for ammonia synthesis on transition metal catalyst supported on  $\text{BaCeO}_{3-x}\text{N}_y\text{H}_z$  where anion vacancies and lattice  $\text{N}^{3-}$  and  $\text{H}^-$  participate in the reaction. Reproduced with permission.<sup>[82]</sup> Copyright 2019, American chemical society.

the dissociative adsorption of  $\text{N}_2$  but instead the formation of N–H bonds on the catalyst surface.<sup>[82]</sup> This new mechanism is highlighted in **Figure 4** with two different pathways proposed and shown alongside the conventional pathway. Instead of the  $\text{H}_2$  and  $\text{N}_2$  reacting on the transition metal catalyst surface, as is the case when supported on  $\text{BaCeO}_3$ , the anion vacancies in the oxyhydride-nitride support mediate the Mars-van Krevelen mechanism.<sup>[82]</sup> As shown in Figure 4, for both proposed mechanisms, lattice  $\text{N}^{3-}$  and  $\text{H}^-$  participate in the reaction.

Recently the use of an Fe catalyst supported on  $\text{CeO}_2$  was shown to exhibit excellent activity at the extremely low temperature of  $100^\circ\text{C}$  when the catalyst bed was exposed to an electric field.<sup>[83]</sup> At atmospheric pressure and  $100^\circ\text{C}$ , the low-Fe-content 7% Fe– $\text{CeO}_2$  catalyst exhibited an activity of  $155\ \mu\text{mol g}^{-1}\text{ h}^{-1}$ . Other catalysts with the same weight percentage on  $\text{CeO}_2$  were also tested, including Ru, Ni, Co, Pd, and Pt, all of which showed activity at this low temperature; however, the Fe catalyst displayed the highest activity. Conventionally when used in a low weight percentage with a catalyst support, Ru catalysts outperform Fe by a significant margin with conventional Fe catalysts using a large weight percentage of Fe. This was shown by Murakami et al.<sup>[83]</sup> when the same catalysts were tested at  $450^\circ\text{C}$  without an applied electric field, with the Ru-based catalyst showing an activity six times higher than that of the Fe catalyst. From this it can be seen that although beneficial to all catalysts at low temperature, the applied electric field has an enhanced effect toward Fe catalysts. The associated mechanism was proposed for ammonia synthesis in an electric field, with density functional theory (DFT) calculations revealing that the  $\text{N}_2\text{H}$  formation step was the limiting step. Their DFT calculations showed that the lowest  $\text{N}_2\text{H}$  formation energy can be attributed to Fe, which is in good agreement with their results.

In a recent report by our group the beneficial effect of oxygen vacancies and the resulting strong metal support interaction (SMSI) effect that occurs was reported for an Fe catalyst promoted with  $\text{Ce}_{0.8}\text{Sm}_{0.2}\text{O}_{2-\delta}$ .<sup>[84]</sup> This catalyst exhibited good activity at  $450^\circ\text{C}$  and 1 MPa of  $8.7\ \text{mmol g}^{-1}\text{ h}^{-1}$  while showing excellent tolerance toward oxygenate poisoning. When 150 ppm of injected known  $\text{O}_2$  was introduced into the feed gas stream, our catalyst retained 47.4% of its activity, whereas industrial wüstite and magnetite only retained 26.4% and 7.6%, respectively.<sup>[84]</sup>

Table 1 highlights the activities of a range of iron catalysts at various reaction conditions and iron contents.

### 3.3. Stability of Iron Catalysts

Stability of Fe-based catalysts is important in achieving long-term operation. The effect of oxygen poisoning in ammonia synthesis catalysts was investigated by Fastrup and Nygard Nielsen in 1992.<sup>[85]</sup> The theory of oxygen poisoning has been discussed at length by Nielsen et al.<sup>[86]</sup> with the theory that an equilibrium coverage of oxygen will be converted to water after some time establishing on the surface. For industrial ammonia catalysts promoted with potassium, the effect of oxygen poisoning is even more pronounced, as reported in 1926.<sup>[87]</sup> In their experiments Fastrup et al. used  $\text{H}_2$  and  $\text{N}_2$  gas of 99.9999% purity with a further purification unit installed and a multiply promoted industrial iron catalyst. In their first experiment, they started ammonia synthesis at  $350^\circ\text{C}$  and 1.5 atm, achieving a stable  $\text{NH}_3$  outlet concentration of around 0.12%. After around 3 h the purification unit was bypassed and it was noted that the ammonia outlet concentration linearly decreased to around

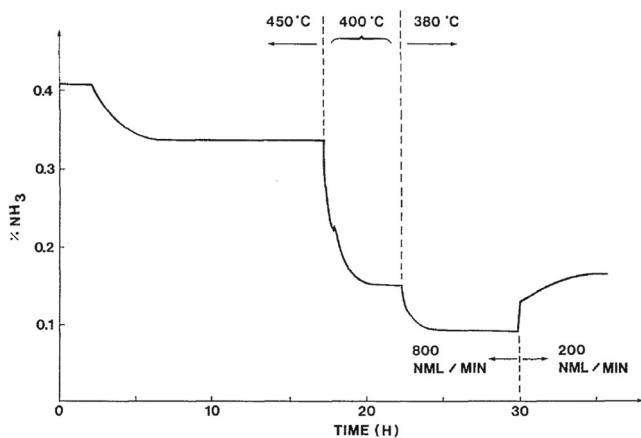


**Figure 5.** Variation in  $\text{NH}_3$  signal when 1.6 ppm of oxygen is added at the 2 h mark to reactant gas at  $450^\circ\text{C}$  and 0.2 MPa. Reproduced with permission.<sup>[85]</sup> Copyright 1992, Springer Nature.

0.08% over 30 h (Figure 5).<sup>[85]</sup> Their next experiment involved increasing the reactor pressure to 2 atm and temperature to  $450^\circ\text{C}$  and adding 1.6 ppm of oxygen to the stream after 2 h. This caused the outlet  $\text{NH}_3$  concentration to drop from around 0.41% to 0.34% over a time of roughly 3 h.<sup>[85]</sup> From this it can be seen that the equilibrium surface coverage of oxygen is reached much faster, which is to be expected. To investigate the claims about the potassium promoter and its susceptibility to oxygen poisoning, they tested two catalysts: one with and one without potassium. By running experiments at 90 bar and  $410^\circ\text{C}$ , they found that in the oxygen-free feed the potassium proved more active with an outlet concentration of 9.6% compared to 7.4% for the potassium-free catalyst.<sup>[85]</sup> However, at the same conditions (90 bar and  $410^\circ\text{C}$ ), when 8 ppm of oxygen was introduced to the feed it was seen that the outlet concentration of the potassium-promoted catalyst dropped to 5.2%, whereas that of the potassium-free catalyst only dropped to 6.9%.<sup>[85]</sup> These results clearly agree with previously reported results.<sup>[87]</sup> That means oxygen can poison iron-based catalysts. Recently it has been reported that oxygen levels of as low as 1 ppm can lead to activity loss in multipromoted fused-iron catalysts.<sup>[88]</sup>

For the production of green ammonia based on the Haber–Bosch process, the presence of oxygenates such as  $\text{O}_2$ ,  $\text{H}_2\text{O}$ , and  $\text{CO}_2$  is inevitable in the feed gases,  $\text{H}_2$  from the electrolysis of water and  $\text{N}_2$  from air separation. Heavy gas purification processes must be adopted to clean the feed gases enough before delivery to the reactor to avoid poisoning of the Fe-based catalysts. If an oxygenate-tolerant catalyst is successfully developed, the requirements on oxygenate removal will be lower and thus less expensive gas purification facilities with reduced energy inputs can be used, improving the overall efficiency. In terms of efficiency, the Haber–Bosch process is suitable for large-scale synthesis plants. However, most green ammonia synthesis plants will be based on locally generated renewable electricity from wind and solar energy and thus will operate at a relatively small scale. To make the localized green ammonia production more efficient, one possible strategy is to increase the overall efficiency by simplifying the gas purification process, which is achievable through the use of oxygenate-tolerant catalysts.

For a catalyst to work the reactants are required to adsorb on to free active sites to make the reaction happen. However, when other substances are present in the reaction a preferential adsorption of those substances on to the free adsorption sites may occur and form strong chemical bonds, causing a drop in catalytic activity or a complete loss altogether, as well as a drop in selectivity.<sup>[89,90]</sup> In ammonia synthesis the poisoning compounds are commonly  $\text{CO}_2$ ,  $\text{CO}$ , and  $\text{H}_2\text{O}$  as well as sulfur, phosphorus, arsenic, and chlorine.<sup>[2]</sup> It has been reported that the total content of  $\text{CO} + \text{CO}_2$  in the inlet to a large scale plant is  $\leq 10 \text{ mg m}^{-3}$  and  $\leq 25 \text{ mg m}^{-3}$  for smaller-scale plants.<sup>[91]</sup> Oxygen and oxygen-containing compounds (oxygenates) can oxidize the commonly used iron catalyst, which leads to the formation of iron oxide crystallites, which causes a loss of surface area.<sup>[92]</sup> However, this process is reversible with the introduction of hydrogen gas to reduce the catalyst, although irreversible grain growth can occur.<sup>[92]</sup> The poisoning effect of oxygenates is particularly bad at lower temperatures and is one of the key issues facing current ammonia synthesis catalysts, where the main drive is to lower the reaction temperature.<sup>[93]</sup> In our study, it was found that deliberate introduction of anion vacancies in the promoter/cocatalyst can significantly improve the oxygenate tolerance of Fe and other metal-based catalysts for the Haber–Bosch process.<sup>[84]</sup>

#### 4. Ruthenium-Based Catalysts

After multipromoted fused-iron catalysts, supported ruthenium catalysts are the second most common ammonia synthesis catalyst and the only other to be used industrially for ammonia synthesis. The Kellogg advanced ammonia process was developed in 1980 and uses ruthenium supported on graphite carbon as the catalyst.<sup>[2]</sup>

Since 1979, when Ru was first supported on graphite carbon and used as an ammonia synthesis catalyst, it has gained a large portion of the research attention for ammonia synthesis catalysts, with a large number of different support materials investigated.<sup>[2,12,94–96]</sup> As well as support materials, Ru loading percentage, precursor form, and impregnation method have also been investigated to determine their effect on catalyst activity. The activities of the most effective current Ru-supported catalysts are reported subsequently. More details on ruthenium catalysts can be found in an early review reported by Saadatjou et al.<sup>[12]</sup>

A major breakthrough in Ru-based catalysts was the classification of the  $\text{B}_5$ -type site as the active site for Ru-based catalysts.<sup>[97]</sup> This site is composed of three Ru atoms in a layer above which there is a layer composed of two Ru atoms. A geometric model can be used to calculate the optimal Ru particle size required to maximize the amount of  $\text{B}_5$ -type sites, with a Ru particle size of 2 nm found to be optimal.<sup>[97]</sup> By performing detailed reduction experiments, Bielawa et al. found that particle growth will increase for the Ru with reduction temperature; therefore, the reduction temperature is key to achieving the required optimal particle size to maximize the number of  $\text{B}_5$  sites.<sup>[97]</sup> As well as the reduction temperature, the barium promoter in Ru catalysts can increase the number of  $\text{B}_5$ -type sites in the Ru catalyst through a reconstruction of the Ru catalyst's surface. By examining the reaction orders of a barium-promoted and unpromoted Ru catalyst, it was found that they were within the experimental



limits, showing the same type of active site is used in both catalysts.<sup>[97]</sup> Therefore, the increased activity in the Ba-promoted Ru catalyst is through an increase in the number of B<sub>5</sub>-type active sites.

Similar to Fe-based catalysts, Ru-based catalysts are also unstable in the presence of trace amounts of oxygenates. At 350 °C and 3 MPa, the ammonia formation rate of the 5 wt% Ru/La<sub>0.5</sub>Ce<sub>0.5</sub>O<sub>1.75</sub> catalyst decreased by over 50% in 20 h when using research-grade H<sub>2</sub> and N<sub>2</sub> (>99.99%) as feed gases, containing low concentrations of oxygenates such as H<sub>2</sub>O, O<sub>2</sub>, and CO<sub>2</sub>.<sup>[77]</sup>

Since the publication of the review article by Saadatjou et al., several new ruthenium catalyst systems have been reported. Wang et al. recently synthesised ZrO<sub>2</sub> and ZrO<sub>2</sub>-KOH supports for ruthenium to be used as an ammonia synthesis catalysts.<sup>[95]</sup> They did this using a similar method to that of Chuah et al.<sup>[98]</sup> where 1 mol L<sup>-1</sup> KOH was added dropwise to ZrO(NO<sub>3</sub>)<sub>2</sub> solutions until a pH of 10.5 was observed. This hydrogel was split, with one being digested in the mother solution at 369 K for 24 h to produce ZrO<sub>2</sub>-KOH and the other aged at room temperature for 24 h to produce ZrO<sub>2</sub>.<sup>[95]</sup> The K-promoted Ru catalyst was added to the support via the wet impregnation method using a solution of K<sub>2</sub>RuO<sub>4</sub>, which was then reduced in ethyl alcohol and treated with H<sub>2</sub> at 723 K for 4 h.<sup>[95]</sup> The Ru/ZrO<sub>2</sub>-KOH catalyst has the highest rate and NH<sub>3</sub> concentration of the catalysts tested, with it being reported that this is due to the high surface area of the ZrO<sub>2</sub>-KOH support compared to other common oxide supports such as Al<sub>2</sub>O<sub>3</sub> and the strong basicity after KOH loading.<sup>[95]</sup>

The use of a carbon-covered Mg-Al hydrotalcite (CCHT) as a ruthenium support was reported by Narasimharao et al.<sup>[99]</sup> in 2015. The Mg-Al hydrotalcite support with a Mg/Al ratio of 2 was prepared by a coprecipitation method under supersaturation conditions. Carbon was coated on the support through pyrolysis of cyclohexene at 873 K. In their results they found that when promoted with cesium and barium with a ruthenium to promoter to support weight ratio of 10/25.5/25.5/100 an ammonia conversion of 0.9% can be achieved at ambient pressure and 600 K.<sup>[99]</sup>

The support morphology as well as synthesis and treatment methods can be shown to have a great effect on the activity of the catalyst. In Table 2, numerous ceria-supported Ru catalysts reported by a number of groups are listed, all highlighting different activities due to the effects that support treatment of morphology have on the catalysts. Lin et al.<sup>[100]</sup> investigated the effect of ceria morphology by synthesizing both ceria rods and ceria cubes to be used as supports. When they tested these supports under the same conditions (1 MPa, 400 °C), they found that the ceria rods gave an activity more than twice that of the ceria cubes (18 mmol g<sup>-1</sup> h<sup>-1</sup> vs 7.9 mmol g<sup>-1</sup> h<sup>-1</sup> at 400 °C and 1 MPa). They noted that the ceria rods have a higher number of oxygen vacancies than the ceria cubes as well as finding a lower crystallinity and higher dispersion of the Ru catalyst on the ceria rods.<sup>[100]</sup> Further work on ceria supports was conducted by Wang et al.<sup>[101]</sup> in which Ru@CeO<sub>2</sub> core-shell particles were synthesized for ammonia synthesis, with Ru cores surrounded by CeO<sub>2</sub> shells. This again had a drastic effect on activity, with an increase from 4 to 8.5 mmol g<sup>-1</sup> h<sup>-1</sup> for the core-shell catalyst when compared to a conventionally supported Ru/CeO<sub>2</sub> catalyst under the same conditions (1 MPa, 425 °C). By forming a

core-shell catalyst structure, they significantly increased ruthenium and support interactions leading to this higher activity.<sup>[101]</sup>

The vast majority of ruthenium catalysts involve a large-weight-percentage support material with ruthenium particles located on the support surface; however, recently catalysts incorporating ruthenium into the support compound have been investigated. Wang et al.<sup>[102]</sup> used perovskite support LaCoO<sub>3</sub> but instead of adding ruthenium to the support surface, they added it as a B-site dopant to get LaCo<sub>0.98</sub>Ru<sub>0.02</sub>O<sub>3</sub>. When this was compared to a conventionally supported Ru catalyst on LaCoO<sub>3</sub> at the same conditions (1 MPa, 450 °C), the activity increased from 4.9 to 10.5 mmol g<sup>-1</sup> h<sup>-1</sup> for the doped perovskite. By substituting Co with Ru, then, a strongly synergistic effect can be achieved for these two species, both of which show activity for ammonia synthesis. This was found to benefit the dissociative adsorption of N<sub>2</sub> through the formation of more Ru clusters along with a larger Co surface presence.<sup>[102]</sup> Other catalysts to use this design include intermetallic YRu<sub>2</sub> synthesized by Ogawa et al.,<sup>[103]</sup> showing an activity 300 times higher than Ru for ammonia synthesis. This significant promotion was attributed to strong electron promotion and a resistance to hydrogen poisoning.<sup>[103]</sup> Despite the significant increase in activity achieved over bulk Ru, it should still be noted that it is not as high as the best performing supported ruthenium catalysts while using a much larger Ru content, ≈70 wt%, greatly increasing the catalyst cost.<sup>[103]</sup> Therefore, the application of YRu<sub>2</sub> on its own is commercially unviable. However, the substitution of Ru with YRu<sub>2</sub> on the best performing support materials may provide a new class of catalysts with significant activity.

Metal hydrides, similar to those discussed for iron catalysts, have been investigated for use as ammonia synthesis catalysts. Kobayashi et al.<sup>[104]</sup> supported a ruthenium catalyst on TiH<sub>2</sub> to be used for ammonia synthesis. Despite reporting a modest activity, their conclusion that the H<sub>2</sub> reactant may exchange with lattice hydrogen provides an interesting development for catalyst design.<sup>[104]</sup> Hattori et al.<sup>[105]</sup> used CaH<sub>2</sub> as the support material with and without the addition of BaO. Their results display significant activity for both catalysts at atmospheric pressure and low temperature (340 °C). When compared to the activity of the Ru/TiH<sub>2</sub> catalyst, there is a significant increase despite the much milder conditions, with activities of 2.8 mmol g<sup>-1</sup> h<sup>-1</sup> for the Ru/TiH<sub>2</sub> catalyst at 400 °C and 5 MPa<sup>[104]</sup> and 7.4 mmol g<sup>-1</sup> h<sup>-1</sup> for the Ru/CaH<sub>2</sub> catalyst at 340 °C and 0.1 MPa.<sup>[105]</sup> This activity is increased even further to 10.5 mmol g<sup>-1</sup> h<sup>-1</sup> when BaO is added to the catalyst support. It is reported that the CaH<sub>2</sub> will facilitate the transformation of BaO to metal hydride BaH<sub>2</sub>, facilitating enhanced electron donation abilities.<sup>[105]</sup> This drastic jump in activity by changing the metal hydride support highlights this as an interesting area of catalyst development with the potential for further enhancement.

Using the findings highlighted earlier, Kitano et al.<sup>[106]</sup> developed core-shell Ru/Ba-Ca(NH<sub>2</sub>)<sub>2</sub> catalysts in which the dispersion of Ba and Ca species appears on the Ru catalyst. By providing good resistance to hydrogen poisoning along with enhanced electronic promotion through the core-shell structure and metal amide support, they achieved excellent activity at mild conditions with a reported value of 60.4 mmol g<sup>-1</sup> h<sup>-1</sup> at 360 °C and 0.9 MPa.<sup>[106]</sup> Similar to the results reported for BaO-CaH<sub>2</sub> where BaH<sub>2</sub> is formed during the catalyst pretreatment and

**Table 2.** Chemical composition and activity of selected ruthenium catalysts for ammonia synthesis.

Catalyst	Ru content [wt%]	Promoters	Reactor temperature [°C]	Reactor pressure [MPa]	Weight hourly space velocity [mL g <sup>-1</sup> h <sup>-1</sup> ]	NH <sub>3</sub> percent in reactor outlet [v/v%]	NH <sub>3</sub> synthesis rate [μmol g <sup>-1</sup> h <sup>-1</sup> ]	Ref.
Ru/CaFH	12	–	50	0.1	36 000	–	50	[107]
Ru/MgO (microwave-assisted 2.45 GHz)	10	–	320	0.1	3000	–	613	[108]
Ru/Cs/Ba/CCHT	6.2	Ba (15.8 wt%) Cs (15.8 wt%)	327	0.1	66 666	0.9	–	[99]
Ru/HT-C12A7:e <sup>-</sup>	2	–	340	0.1	18 000	–	2290	[96]
Ru/BaO–CaH <sub>2</sub>	10	–	340	0.1	36 000	–	10 500	[105]
Ru/CaH <sub>2</sub>	10	–	340	0.1	36 000	–	7400	[105]
K/Ru/graphite	10	K (2 wt%)	400	0.1	–	–	490	[161]
Ru/HT–C12A7	2	–	400	0.1	36 000	–	3050	[162]
Ru/SAs/S-1	0.27	Ba (9 wt%)	400	0.1	18 000	–	1389.5	[163]
YRu <sub>2</sub>	–	–	400	0.1	18 000– 36 000	–	3318	[103]
Ru/BaZrO <sub>3</sub>	2	–	400	0.1	36 000	–	3630	[164]
Ru/BaZr <sub>0.9</sub> Y <sub>0.1</sub> O <sub>3</sub>	2	–	400	0.1	36 000	–	4000	[164]
Ru/graphene	1.4	Ba/Ru = 1	400	0.1	36 000	–	336	[165]
Ru/2.0SrNb	2	Cs/Ru = 8	450	0.1	36 000	–	5035	[166]
Ru/Sibunit	4	Ba (10.8 wt%) Cs (2.6 wt%)	350	0.7	–	–	1540	[167]
Ru/Ca(NH <sub>2</sub> ) <sub>2</sub>	10	–	300	0.8	36 000	–	15 800	[116]
Ru/Ba–Ca(NH <sub>2</sub> ) <sub>2</sub>	10	Ba (3 at%)	360	0.9	36 000	–	60 400	[106]
Ru/BaCeO <sub>3-x</sub> H <sub>y</sub> N <sub>z</sub> (after 20 h)	4.5	–	400	0.9	36 000	–	28 570	[82]
Ru/mesoporous carbon(MPC)-18	13.8	Cs/Ru = 1.1	360	0.99	–	–	10 200	[168]
Ru/MPC	10	Cs (33 wt%)	370	0.99	–	–	8100	[169]
Ru/MPC	10	Ba/Ru = 0.5	380	0.99	–	–	10 400	[170]
Ru/Ce <sub>0.5</sub> La <sub>0.5</sub> O <sub>1.75</sub>	5	–	350	1	72 000	–	31 300	[77]
Ru/Pr <sub>2</sub> O <sub>3</sub>	5	–	400	1	18 000	–	19 000	[171]
Ru/Ti–Ce–S	3	–	400	1	–	–	14 580	[172]
Ru/Yttria Stabilized Zirconia (YSZ)	0.4–1.0	Ba/Ru=1	400	1	72 000	–	5640–14 100	[173]
Ru/gC–Al <sub>2</sub> O <sub>3</sub>	5	Ba (6 wt%)	400	1	60 000	–	5611	[174]
Ru/Al <sub>2</sub> O <sub>3</sub> -980	5	Ba (6 wt%)	400	1	60 000	–	7217	[175]
Ru/La <sub>0.5</sub> Pr <sub>0.5</sub> O <sub>1.75</sub>	5	–	400	1	72 000	–	60 200	[176]
Ru/MgO–MIL	3.1	Cs/Ru = 1	400	1	24 000	–	22 290	[177]
Ru/CeO <sub>2</sub> -r	4	–	400	1	18 000	–	3830	[178]
Ru/CeO <sub>2</sub> -c	4	–	400	1	18 000	–	1289	[178]
Ru@CeO <sub>2</sub> -9	2.48	–	425	1	60 000	–	8500	[101]
LaCo <sub>0.98</sub> Ru <sub>0.02</sub> O <sub>3</sub>	0.93	–	450	1	–	–	10 500	[102]
Ru/MgO	2	Cs (6.4 wt%)	400	2.6	–	–	4200	[179]
Ba/Ru/Graphitic Nanofilaments (GNFS)	4	Ba (1 wt%)	400	3.0	–	–	18 570	[180]
Ru/BaCeO <sub>3</sub>	3	–	400	3.0	–	–	6450	[181]
Ru/ZrO <sub>2</sub> –KOH	–	–	400	3.0	–	3.95	11 100	[95]
Ru/Pr <sub>2</sub> O <sub>3</sub>	5	–	400	3	72 000	–	64 000	[182]
Ru/Y–layered double oxide (LDO)	3.85	–	425	3	–	–	16 120	[183]
Ru/MgAl–LDO	3.86	–	425	3	–	–	14 760	[183]
Ru/BaCeO <sub>2</sub> -a	1.25	Cs (4%)	450	3.0	24 000	–	28 000	[184]
Ru/CeO <sub>2</sub> –C <sub>12</sub> H <sub>29</sub> NO (TPAOH)	2.5	Cs (4%)	450	3	24 000	–	32 000	[185]

**Table 2.** Continued.

Catalyst	Ru content [wt%]	Promoters	Reactor temperature [°C]	Reactor pressure [MPa]	Weight hourly space velocity [mL g <sup>-1</sup> h <sup>-1</sup> ]	NH <sub>3</sub> percent in reactor outlet [v/v%]	NH <sub>3</sub> synthesis rate [μmol g <sup>-1</sup> h <sup>-1</sup> ]	Ref.
Ru/CeO <sub>2</sub> -CS	2.5	–	450	3	70 000	–	27 000	[186]
Ru/Li/AC	4.8	Li (7.6 wt%) Ba (5.25 wt%)	460	3	62 400	–	106 120	[187]
Ru/CeO <sub>2</sub> -MS	2.5	Ba (6%)	450	3.8	24 000	–	24 000	[188]
Ru/Al <sub>2</sub> O <sub>3</sub>	4	–	400	5.0	–	–	390	[94]
Ru/MgO	4	–	400	5.0	–	–	7390	[94]
Ru/BaTiO <sub>3</sub>	4	–	400	5.0	–	–	15 670	[94]
Ru/TiH <sub>2</sub>	0.9	–	400	5	66 000	–	2800	[104]
Ru/BaTiO <sub>2.5</sub> H <sub>0.5</sub>	0.9	–	400	5	66 000	–	1400	[104]
Ru/BaTiO <sub>2.5</sub> H <sub>0.5</sub>	1	–	400	5	36 000	–	28 200	[81]
BaCs–RuC (N <sub>2</sub> )	–	Ru:Ba:Cs 1:0.05:0.2	400	9.5	–	–	287 647	[189]
Ru/CeO <sub>2</sub> -r	10	–	400	10	70 000	–	115 000	[100]
Ba/Ru/BN	4.5	Ba (5.6 wt%)	400	10	–	–	186 600	[190]
Ru–N–mesoporous carbon (MC)	3.75	Ba (4 wt%)	400	10	–	–	79 000	[191]
Ru/MC	2.3	Ba(4%) K(14%)	400	10	–	–	133 000	[192]
Ru/AC-G	10	Ba(9 wt%)	400	10	70 000	–	312 500	[109]
Ru/La <sub>2</sub> Ce <sub>2</sub> O <sub>7</sub>	4	–	425	10	–	12.94	52 700	[193]
Ru/carbon nanotubes (CNT)-D	3.4	Ba (3.4 wt%)	450	10	–	–	110 000	[194]

reaction,<sup>[105]</sup> Ba(NH<sub>2</sub>)<sub>2</sub> is reportedly formed, resulting in a promotion toward the dissociative adsorption of N<sub>2</sub>, thereby shifting the rate-limiting step.<sup>[106]</sup>

Extremely low-temperature ammonia synthesis from H<sub>2</sub> and N<sub>2</sub> has been recently demonstrated using a Ru-based catalyst by Hattori et al.<sup>[107]</sup> Solid solution CaFH was used as the Ru catalyst support with an activity of 50 μmol g<sup>-1</sup> h<sup>-1</sup> achieved at ambient pressure and a near-ambient temperature of 50 °C. CaFH support can be formed at low temperature from the solid solution of CaF<sub>2</sub> and CaH<sub>2</sub>; the weak ionic bonds in this solid solution between Ca<sup>2+</sup> and H<sup>-</sup> were attributed to the excellent catalytic performance by Hattori et al.,<sup>[107]</sup> with the H<sup>-</sup> sites facilitating the release of hydrogen atoms.

Microwave-assisted ammonia synthesis was reported by Wildfire et al.<sup>[108]</sup> using a Ru/MgO catalyst. An activity of 613 μmol g<sup>-1</sup> h<sup>-1</sup> was reported at 320 °C and ambient pressure in a 2.45 GHz microwave reactor. They noted that the Ru loading had a significant impact on this synthesis method with a lower metal site temperature and quicker response time when the loading percentage of Ru increased from 4% to 10%. Although the reported activity is not as high as the current best performing Ru catalysts under conventional conditions, the demonstration of this technology with Ru/MgO may open this synthesis method up to other higher activity Ru-based catalysts.

The properties of typical reported Ru-based ammonia synthesis catalysts are listed in Table 2. The highest NH<sub>3</sub> formation rate of 310 000 μmol g<sup>-1</sup> h<sup>-1</sup> at 100 bar and 400 °C was observed for the Ba-promoted Ru catalyst supported on AC-G when a WHSV of 70 000 mL g<sup>-1</sup> h<sup>-1</sup> was used.<sup>[109]</sup> Although this activity appears high, the flow rate used for their catalytic activity test was relatively high at 70 dm<sup>3</sup> h<sup>-1</sup>. When considering the flow

rate, the highest activity is seen for Ru/Ba–Ca(NH<sub>2</sub>)<sub>2</sub>, with 60 400 μmol g<sup>-1</sup> h<sup>-1</sup> at 9 bar and 360 °C, which was achieved at the much lower flow rate of 3.6 dm<sup>3</sup> h<sup>-1</sup> corresponding to a much higher conversion.<sup>[106]</sup> Metal hydrides, amides, and oxyhydrides have proven to be excellent support materials for the Ru ammonia synthesis catalysts that can provide protection against hydrogen poisoning and in some cases, shift the rate-limiting step. At ambient pressure, Ru supported on high-surface-area 12CaO·7Al<sub>2</sub>O<sub>3</sub> electride exhibits the highest catalytic activity, with a value of 2290 μmol g<sup>-1</sup> h<sup>-1</sup> at a temperature of only 340 °C.<sup>[96]</sup>

Although the Ru-based catalysts exhibit exceptionally high activity toward ammonia synthesis at reduced temperature and pressure, in 2017, the global ruthenium production was reported at 35.5 tonnes.<sup>[110]</sup> If an ammonia synthesis plant needs 300 tonnes of a catalyst, in which the said catalyst contains only 2 wt% Ru, then 6 tonnes of Ru will be required, roughly 17% of the global annual Ru production. This will result in a sharp increase in the price of Ru. Therefore, globally there are approximately only ten ammonia synthesis plants that use Ru-based catalysts, while the rest of the market is dominated by the cheap fused-Fe-based catalysts.

## 5. Electride-Based Catalysts

Although part of the supported ruthenium class of catalysts reported previously, ruthenium catalysts with electride supports are discussed in more detail due to the excellent promotion effect of this recent material.

Recently electride-based catalysts commonly using the electride material as the catalyst support have gained attention. An electride is an O<sup>2-</sup> ionic compound in which electrons act

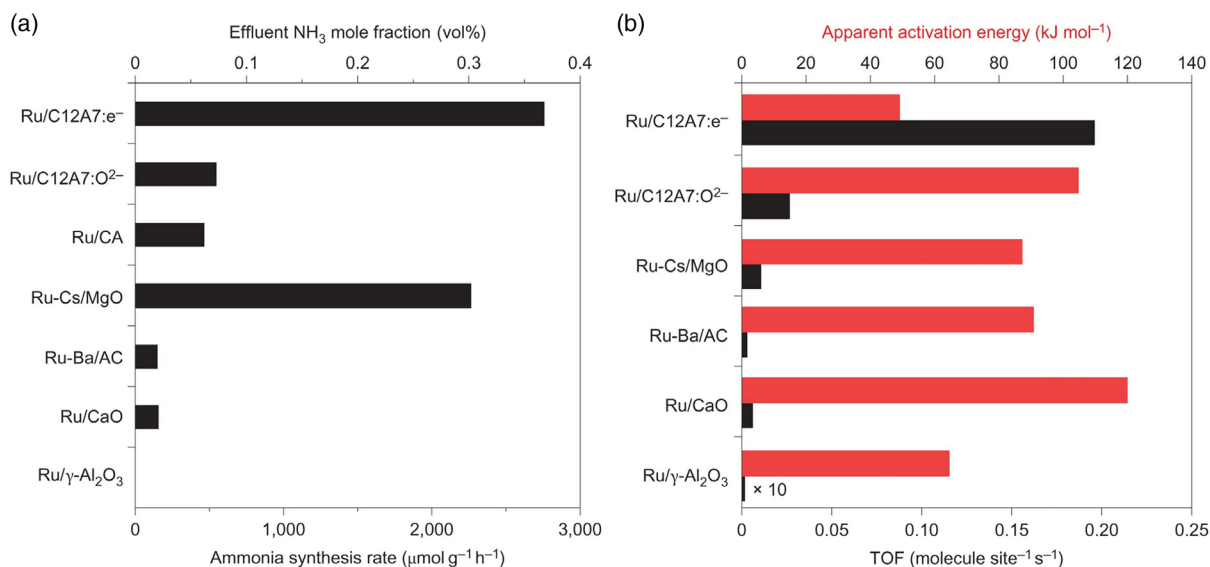


**Figure 6.** a) Ammonia synthesis rate and outlet ammonia mole fractions for Ru/C12A7:e<sup>-</sup> compared with various supported Ru catalysts. b) Apparent activation energy and turnover frequency for Ru/C12A7:e<sup>-</sup> compared with various supported Ru catalysts. All catalysts were loaded with 1 wt% Ru and tested at 0.1 MPa, 400 °C, H<sub>2</sub>/N<sub>2</sub> = 3, 60 mL min<sup>-1</sup>. Reproduced with permission.<sup>[7]</sup> Copyright 2012, Springer Nature.

as the anion.<sup>[111,112]</sup> The majority of these complexes are organic and have poor thermal stability. This led to the development of the inorganic electride with the formula  $[\text{Ca}_{24}\text{Al}_{28}\text{O}_{64}]^{4+}(\text{e}^-)_4$  in 2003, which showed good stability above room temperature.<sup>[113]</sup> This electride was investigated as a support material by Inoue et al.<sup>[7,96]</sup> due to its strong electron-donating ability and hydrogen storage ability. The immediate benefits of this catalyst support can be seen in **Figure 6**, where the activity, ammonia outlet mole fraction, activation energy, and turnover frequency are reported alongside conventional supported ruthenium catalysts all at 0.1 MPa and 400 °C.<sup>[7]</sup> In terms of activity, only the cesium-promoted Ru/MgO catalyst comes close, while for turnover frequency the Ru/ $[\text{Ca}_{24}\text{Al}_{28}\text{O}_{64}]^{4+}(\text{e}^-)_4$  catalyst dwarfs the others.

They synthesized the support material using two different methods, the solid phase reaction method and the hydrothermal method.<sup>[7,96]</sup> The temperature at which water and hydroxyl groups were removed during the hydrothermal synthesis was varied between 873 and 1273 K to find out how this affected the surface area and catalytic performance.<sup>[96]</sup>  $[\text{Ca}_{24}\text{Al}_{28}\text{O}_{64}]^{4+}(\text{e}^-)_4$  synthesized using the hydrothermal method at 1173 K produced the highest rate for ammonia synthesis for the electride-supported catalysts, which is higher than that of K-Ru/Al<sub>2</sub>O<sub>3</sub> and Ru/ZrO<sub>2</sub> at the same temperature and pressure (3 MPa).<sup>[95]</sup> It is also higher than that of the Ru-Cs/MgO catalyst at the same temperature and pressure.<sup>[96]</sup> The structure of the  $[\text{Ca}_{24}\text{Al}_{28}\text{O}_{64}]^{4+}(\text{e}^-)_4$  electride is shown in **Figure 7**, where the green sphere represents the possible space electrons can occupy in the structure.

Further research into electride materials led to the finding that in the Ru/HT-C12A7:e<sup>-</sup> catalyzed reaction, the nitrogen dissociation step was no longer the rate-limiting step and that the new rate-limiting step was due to the formation of the NH<sub>n</sub><sup>\*</sup> species as shown in Equation (4)–(6).<sup>[114]</sup> This discovery then further increased interest in new electride materials for ammonia synthesis.

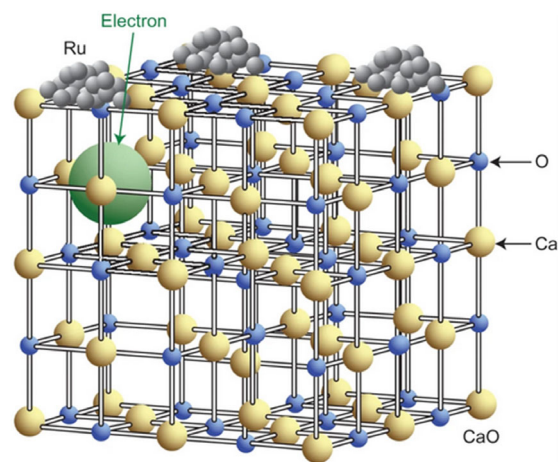


**Figure 7.** Lattice structure of the  $[\text{Ca}_{24}\text{Al}_{28}\text{O}_{64}]^{4+}(\text{e}^-)_4$  electride with Ru loading. The structure shows how electrons occupy the oxygen vacancies in the material. Reproduced with permission.<sup>[7]</sup> Copyright 2012, Springer Nature.

Following their work on C12A7:e<sup>-</sup>, Inoue et al.<sup>[115]</sup> investigated the 2d electride Ca<sub>2</sub>N:e<sup>-</sup> as an ammonia catalyst support for the Ru catalyst. They noted stable catalytic activity down to temperatures as low as 200 °C while also providing a notable increase in activity across the temperature range tested. However, it was believed that this increase was due to the hydride Ca<sub>2</sub>NH formed during the reaction and not the electride.<sup>[115]</sup> Inoue et al. further investigated the electride-derived hydride Ca(NH<sub>2</sub>)<sub>2</sub> for its activity toward ammonia synthesis with the Ru catalyst.<sup>[116]</sup>

Recently, the water-stable electride Y<sub>5</sub>Si<sub>3</sub> has been investigated as a Ru support for ammonia synthesis by Lu et al.<sup>[117]</sup> In their work, they exposed the prepared Y<sub>5</sub>Si<sub>3</sub> samples to distilled water for 1 h before measuring the activity. It was observed that the

activity of the sample remained constant between the dry catalyst and the wetted one. This provides a noted advantage when compared to conventional Ru support materials such as MgO while achieving comparable activity.<sup>[117]</sup> Further work on this electride was conducted by Lu et al.<sup>[118]</sup> Y<sub>5</sub>Si<sub>3</sub> ingots were obtained through arc melting as before from their metallic precursors. However, instead of mechanically grinding the obtained ingots, they were treated using Ar/H<sub>2</sub> arc evaporation at a temperature of 1000 °C.<sup>[118]</sup> The evaporated Y<sub>5</sub>Si<sub>3</sub> was flown out of the chamber and filtered to obtain nanoparticles of the electride. This method further emphasizes the effect that the support morphology and particle size has on the catalytic activity as an increase from 1.875 to 4.448 mmol g<sup>-1</sup> h<sup>-1</sup> at 340 °C and 0.1 MPa was achieved when the support was changed from mechanically ground Y<sub>5</sub>Si<sub>3</sub> to Y<sub>5</sub>Si<sub>3</sub> nanoparticles, respectively.<sup>[118]</sup> This increase in activity was also accompanied by a decrease in reaction temperature of 60 °C from 400 to 340 °C with both taking place at atmospheric pressure.

Wu et al. recently noted the potential of LaScSi as an electride support for Ru in the catalytic synthesis of ammonia.<sup>[119]</sup> Again, like Y<sub>5</sub>Si<sub>3</sub>, the electride support was noted to have good stability in air and water while exhibiting good activity with a turnover frequency of 0.1 s<sup>-1</sup> at 0.1 MPa and 400 °C. They attributed its high performance to the nature of its anionic electrons, which were tiered and in higher concentration than other electrides, demonstrating desirable properties for the future of electride-based catalysts.<sup>[119]</sup>

Like the electride LaScSi, LaRuSi was synthesized by Li et al.<sup>[120]</sup> Again, this catalyst was stable in air and water, with stability even reported in some acids such as HNO<sub>3</sub> and Ethylenediaminetetraacetic acid (EDTA). By incorporating Ru into the support lattice rather on the surface, numerous advantages can be achieved, as highlighted in the previous section for the catalysts LaCo<sub>0.98</sub>Ru<sub>0.02</sub>O<sub>3</sub> and YRu<sub>2</sub>.<sup>[102,103]</sup> At the same conditions a slight increase in activity over the supported electride Ru/LaScSi was observed with an activity of 5.34 mmol g<sup>-1</sup> h<sup>-1</sup> obtained for LaRuSi and 5.3 mmol g<sup>-1</sup> h<sup>-1</sup> for Ru/LaScSi,<sup>[120]</sup> both of which were achieved at 400 °C and 0.1 MPa. The observed activation energy of N<sub>2</sub> dissociation on the LaRuSi catalyst was lower than that observed for conventional Ru-supported catalysts and the turnover frequency (TOF) was increased by a

factor of 600 over the Ru powder at their reaction conditions (400 °C and 0.1 MPa).<sup>[120]</sup> By replacing La with Ce in the electride to form CeRuSi that activity can further increase to 5.48 mmol g<sup>-1</sup> h<sup>-1</sup> under the same reaction conditions; CaRuSi was also investigated by Wu et al.<sup>[121]</sup> but performed much worse, with an activity of 0.06 mmol g<sup>-1</sup> h<sup>-1</sup> at these conditions.<sup>[121]</sup> However, it should be noted that although the activity of both LaRuSi and CeRuSi is slightly higher than that of Ru/LaScSi, the weight percentage of Ru in the catalyst is much higher too, with ≈38 wt% Ru in both LaRuSi and CeRuSi but only 8.3 wt% in Ru/LaScSi.<sup>[120]</sup> This will significantly increase the cost, making the realistic application of such catalysts unviable considering the slight increase in activity.

The activities and reaction conditions of various electride-based catalysts are highlighted in Table 3. Although good activity for this interesting class of catalysts has been shown over a variety of different electride materials at low temperatures (≤400 °C), the reaction pressure is 0.1 MPa for all reported catalysts. As the synthesis loop in the KAAP process operates at a pressure of ≈9 MPa while using a conventional ruthenium catalyst supported on activated carbon,<sup>[2]</sup> activity tests of the best performing electrides at these conditions are required to further evaluate their feasibility for industrial application.

## 6. Cobalt-Based Catalysts

In recent years, cobalt-based ammonia synthesis catalysts have attracted the attention of researchers because of their high activity. Like ruthenium, cobalt-based catalysts are commonly used with a support material; however, unlike ruthenium this is solely for promotion effects and is not a cost issue, as is also the case with ruthenium.<sup>[2]</sup> As such, these supports/promoters can be added in a much greater weight percentage range, from a few weight percentage as seen in multipromoted fused-iron catalysts to weight percentages similar to those seen for ruthenium.

In 2002, Hagen et al.<sup>[122]</sup> investigated the catalytic activity of a barium-promoted cobalt catalyst supported on carbon for ammonia synthesis. To synthesize the catalyst, they first cleaned Vulcan XC-72 at 1372 K using 10% H<sub>2</sub> in N<sub>2</sub>. After this, both cobalt and barium were added to the support carbon through incipient wetness impregnation using Co(NO<sub>3</sub>)<sub>2</sub> and Ba(O<sub>2</sub>CCH<sub>3</sub>)<sub>2</sub> as the

**Table 3.** Chemical composition and activity of selected ruthenium catalysts for ammonia synthesis.

Catalyst	Ru content [wt%]	Promoters [wt%]	Reactor temperature [°C]	Reactor pressure [MPa]	WHSV [mL g <sup>-1</sup> h <sup>-1</sup> ]	NH <sub>3</sub> percentage in reactor outlet [v/v%]	NH <sub>3</sub> synthesis rate [μmol g <sup>-1</sup> h <sup>-1</sup> ]	Ref.
Ru/HT-C12A7:e <sup>-</sup>	2	–	340	0.1	18 000	–	2290	[96]
Ru/Ca <sub>2</sub> N:e <sup>-</sup>	1.8	–	340	0.1	36 000	–	3386	[115]
Ru/Ca(NH <sub>2</sub> ) <sub>2</sub>	1.8	–	340	0.1	36 000	–	3386	[195]
Ru/Y <sub>5</sub> Si <sub>3</sub> NP	10	–	340	0.1	36 000	–	4448	[118]
Ru/C12A7 (microcube)	5	–	400	0.1	36 000	–	5380	[196]
Ru/Y <sub>5</sub> Si <sub>3</sub>	7.8	–	400	0.1	18 000	–	1875	[117]
Ru/LaScSi	8.3	–	400	0.1	36 000	0.36	5300	[119]
LaRuSi	–	–	400	0.1	36 000	0.492	5340	[120]
CeRuSi	–	–	400	0.1	36 000	–	5480	[120]
CaRuSi	–	–	400	0.1	36 000	–	60	[121]

metal precursors. They measured the activity of the prepared catalyst using a stainless steel microreactor over the temperature range of 320–440 °C and pressure range of 2–50 bar. From these experiments they found that the highest activity could be obtained at 440 °C and 10 bar with a H<sub>2</sub>/N<sub>2</sub> mole ratio of 3/1; at these conditions a rate of 86 400 μmol g<sup>-1</sup> h<sup>-1</sup> was achieved.

In 2006 Rarog-Pilecka et al.<sup>[123]</sup> investigated the role of the preparation procedure on the catalytic activity of carbon-supported cobalt catalysts for ammonia synthesis. They produced the carbon support by treating activated carbon in helium at 1900 °C followed by CO<sub>2</sub> at 850 °C. This carbon support was then impregnated with cobalt using cobalt nitrate hexahydrate as the precursor. This sample was calcined after drying at 220 °C and labeled “Co/C”; this sample was further treated in hydrogen at 350 °C to create Co<sub>R+P</sub>/C. A third sample was then produced through reoxidizing the Co<sub>R+P</sub>/C at 220 °C in air to produce Co<sub>R+P+C</sub>/C.<sup>[123]</sup> All of these samples were also investigated after impregnation with barium using a barium nitrate precursor. The activity of these catalysts was measured at 9 MPa using a H<sub>2</sub>/N<sub>2</sub> mole ratio of 3/1 over the temperature range of 400–470 °C. In their results they reported that the highest activity was obtained at 470 °C using the Ba–Co<sub>R+P+C</sub>/C catalyst with a rate of 2.17 g<sub>NH<sub>3</sub></sub> g<sup>-1</sup> h<sup>-1</sup>.<sup>[123]</sup>

In 2007 the treatment method of the carbon support for the cobalt catalyst was investigated by Rarog-Pilecka et al.<sup>[124]</sup> The first two supports were prepared from commercial activated carbon with both being treated at 1900 °C in helium, with one of them further treated in CO<sub>2</sub> at 850 °C. A third support was obtained following the same two-step procedure using helium and CO<sub>2</sub> but using GF45 from Norit as the starting material.<sup>[124]</sup> Two different cobalt precursors were used, cobalt nitrate hexahydrate and cobalt acetate, which were both added to the support material through impregnation. Again, barium nitrate was added as a promoter using the standard impregnation method.<sup>[124]</sup> These prepared catalysts were then subjected to the oxidation, reduction, and reoxidation pattern as reported in their previous work.<sup>[123]</sup> When evaluating the catalyst at 9.0 MPa, 400 °C, and a stoichiometric H<sub>2</sub> N<sub>2</sub> gas follow, it was found that the highest activity was for the catalyst supported on the treated GF45 support, with a rate of 1.52 g<sub>NH<sub>3</sub></sub> g<sup>-1</sup> h<sup>-1</sup>.<sup>[124]</sup>

In 2008, Rarog-Pilecka et al.<sup>[125]</sup> again investigated the use of cobalt as an ammonia synthesis catalyst. This time they used activated carbon as a template to form an unsupported cobalt catalyst. Commercial activated carbon after being treated with hydrogen was used as the template material. This was then impregnated using cobalt nitrate both with and without cerium nitrate. This impregnation was repeated until an inorganic-to-carbon weight ratio of 1.5:1 was obtained. The carbon was then burnt off at 250 °C in air. Both the cobalt and cobalt–cerium oxide catalyst obtained this way were promoted with barium using the conventional method.<sup>[125]</sup> When investigating the activity of the produced catalysts, they found that the doubly promoted cobalt catalyst promoted with both cerium and barium had the highest activity with an activity of 1.98 g<sub>NH<sub>3</sub></sub> g<sup>-1</sup> h<sup>-1</sup> when tested at 6.3 MPa and 400 °C with a gas mole ratio of H<sub>2</sub>/N<sub>2</sub> of 3/1.<sup>[125]</sup>

The preparation method of the doubly promoted cobalt catalyst was again investigated by Rarog-Pilecka et al. in 2011 with barium- and cerium-promoted cobalt catalysts prepared through the coprecipitation method.<sup>[126]</sup> To prepare the catalysts, they

added potassium carbonate to an aqueous solution of either cobalt nitrate or cobalt nitrate and cerium nitrate to obtain the cobalt and cerium carbonates. After drying, these carbonates were then treated at 500 °C in air overnight to obtain the oxide catalyst. Again barium nitrate was added as a promoter using the standard impregnation method.<sup>[126]</sup> When evaluating the activity, they used a pressure of 6.2 MPa with a gas mole ratio of H<sub>2</sub>/N<sub>2</sub> of 3/1. Again, the highest activity was for the doubly promoted catalyst, with the highest turnover frequency being 0.370 s<sup>-1</sup> at a temperature of 430 °C.<sup>[126]</sup>

In 2012 the effect of cerium addition was studied by Karolewska et al.<sup>[127]</sup> They synthesized the catalyst through coprecipitation using cobalt nitrate and cerium nitrate with potassium carbonate as the precipitant. From this the carbonates of cerium and cobalt were obtained, which were converted to the oxide catalyst through air treatment at 500 °C. Again barium nitrate was added as a promoter using the standard impregnation method.<sup>[127]</sup> The catalyst activity was measured at 400 °C with a pressure of 6.3 MPa and a gas mole ratio of H<sub>2</sub>/N<sub>2</sub> of 3/1; at these conditions it was found that a cerium loading of 11.5 wt% provided the highest rate, with ammonia produced with a value of 3.33 g<sub>NH<sub>3</sub></sub> g<sup>-1</sup> h<sup>-1</sup>.<sup>[127]</sup>

In 2013 Karolewska et al. further studied the effect of cerium addition and the preparation procedure on cobalt catalysts supported on carbon.<sup>[128]</sup> Their carbon support was obtained from treated commercial activated carbon; the cobalt and cerium were then supported on the carbon following two different procedures.<sup>[128]</sup> The first involved separate impregnation steps for both the cobalt nitrate and cerium nitrate precursors using an alcoholic solution. The second procedure used a coimpregnation method in which both the nitrate precursors were added together. After drying, the samples from both of these procedures were calcined to form the oxide catalyst. Again barium nitrate was added as a promoter using the standard impregnation method.<sup>[128]</sup> Catalytic activity measurements were conducted at 9.0 MPa at a temperature of 400 °C using a stoichiometric gas flow of nitrogen and hydrogen. At these conditions it was found that a higher rate can be achieved when the catalyst is prepared through the coimpregnation method, with a rate of 8.16 g<sub>NH<sub>3</sub></sub> g<sup>-1</sup> h<sup>-1</sup> for the coimpregnated catalyst and 4.95 g<sub>NH<sub>3</sub></sub> g<sup>-1</sup> h<sup>-1</sup> for the stepwise-impregnated catalyst.<sup>[128]</sup>

Recently, Lin et al.<sup>[129]</sup> have prepared a cobalt catalyst supported on ceria for the synthesis of ammonia. They prepared a series of Co/CeO<sub>2</sub> catalysts with a range of different properties of surface hydroxyl groups by varying the pretreatment method. They prepared these catalysts through the coprecipitation method, with an aqueous solution of Ce(NO<sub>3</sub>)<sub>3</sub> and Co(NO<sub>3</sub>)<sub>3</sub> with a weight ratio of Co to CeO<sub>2</sub> of 7.9 wt%. A suspension with pH 10 was then formed by adding NaOH dropwise with this suspension being aged for 3 h. The suspension was washed with distilled water and dried overnight at 110 °C. The obtained catalyst was then either treated with air or hydrogen for 4 h at 600 °C.<sup>[129]</sup> The ammonia formation rates at various temperatures and a pressure of 10 MPa are shown in **Figure 8**. They proposed the reaction pathway shown in **Figure 9**.

In their results they noted that high catalytic activity was observed for catalysts after reduction in hydrogen at a high temperature.<sup>[129]</sup> This could be related to the formation of hydroxyl ions on the surface (**Figure 9**). The OH<sup>-</sup> ions may react with H,

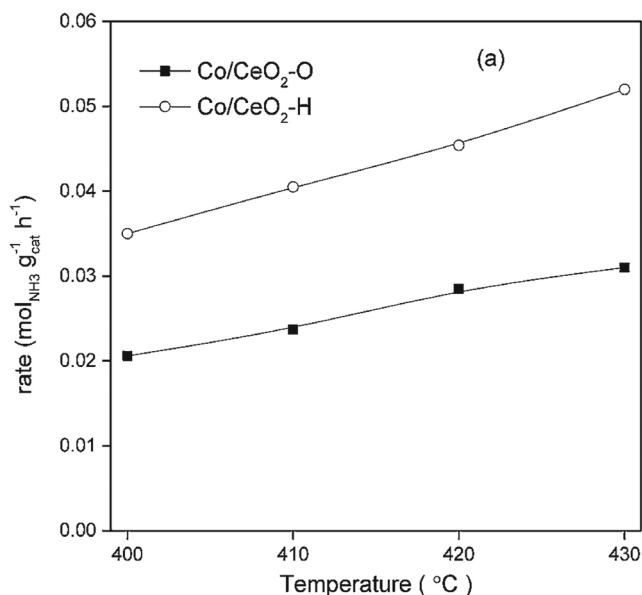


**Figure 8.** Ammonia synthesis rate of Co/CeO<sub>2</sub> at 10 MPa and WHSV 2.5 × 10<sup>5</sup> cm<sup>3</sup> g<sub>cat</sub><sup>-1</sup> h<sup>-1</sup> (O:catalyst pretreated in air, H:catalyst pretreated in hydrogen). Reproduced with permission.<sup>[129]</sup> Copyright 2011, RSC Publishing.

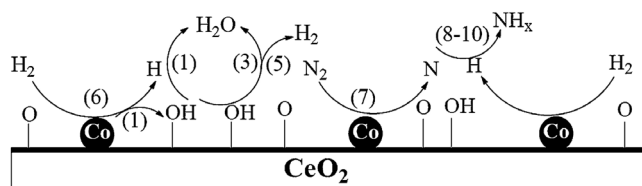


**Figure 9.** Proposed reaction pathway for ammonia synthesis on Co/CeO<sub>2</sub>. Reproduced with permission.<sup>[129]</sup> Copyright 2011, RSC Publishing.

forming H<sub>2</sub>O and thereby leaving the surface, leaving the active site for absorption of nitrogen, which may facilitate the formation of ammonia. In the Ru-based ammonia synthesis catalysts, it was found that the ammonia synthesis catalytic activity of 4 wt% Ru on Sm<sub>2</sub>O<sub>3</sub>-CeO<sub>2</sub> increases with the doping of Sm<sub>2</sub>O<sub>3</sub> and the maximum activity was observed at 7 mol% Sm doping. It was believed that the oxygen vacancies induced by Sm<sup>3+</sup> present in ceria are not only facilitated by the reduction of the surface oxygen of ceria, but also favorable to the hydrogen desorption.<sup>[130]</sup> From this point of view, introduction of oxygen vacancies in the catalyst support/promoter is a good strategy to improve the ammonia synthesis activity.

In 2015 Tarka et al.<sup>[131]</sup> reported on the effect of a barium promoter on the stability and activity for ammonia synthesis when used to promote a carbon-supported cobalt catalyst. The prepared catalysts used in the experiments all had a cobalt content of 27.4 wt%, with the barium promoter content varying from 0 to 0.88 mmol g<sup>-1</sup> (C + Co).<sup>[131]</sup> The catalysts were then tested at 9 MPa, 400 °C with a H<sub>2</sub>/N<sub>2</sub> ratio of 3/1; at these conditions it was found that a barium promoter content of 0.68 mmol g<sup>-1</sup> (C + Co) performed best, with an ammonia synthesis rate of 1.5 g<sub>NH<sub>3</sub></sub> g<sub>C+Co</sub><sup>-1</sup> h<sup>-1</sup> achieved.<sup>[131]</sup>

McAulay et al. reported the activity of a Co-Re catalyst for ammonia synthesis.<sup>[132]</sup> The CoRe<sub>4</sub> catalyst used in their

experiments was synthesized by mixing NH<sub>4</sub>ReO<sub>4</sub> with Co(NO<sub>3</sub>)<sub>2</sub>·6H<sub>2</sub>O in deionized water.<sup>[132]</sup> This mixture was then dried and calcined in air. The catalyst activity was measured at ambient pressure and a temperature of 400 °C with a H<sub>2</sub>/N<sub>2</sub> feed gas ratio of 3/1. At these conditions they reported an ammonia synthesis rate of 943 μmol g<sup>-1</sup> h<sup>-1</sup>.<sup>[132]</sup>

The effect of lanthanum addition on cobalt catalysts obtained through coprecipitation was studied by Zybert et al. in 2015.<sup>[133]</sup> The catalysts were prepared by adding potassium carbonate to an aqueous solution of cobalt nitrate and lanthanum nitrate to form carbonates of cobalt and lanthanum. These were then fired in air to obtain the oxide catalysts, which were then impregnated with barium using the standard method.<sup>[133]</sup> When testing the activity of these catalysts at 430 °C and 6.3 MPa with a H<sub>2</sub>/N<sub>2</sub> feed gas ratio of 3/1, they reported that a rate of 3.27 g<sub>NH<sub>3</sub></sub> g<sup>-1</sup> h<sup>-1</sup> was achieved for the barium- and lanthanum-promoted catalyst.<sup>[133]</sup> **Table 4** shows the activity of a range of cobalt-based catalysts for ammonia synthesis.

In these catalysts, Co supported on CeO<sub>2</sub> or carbon and promoted with Ba exhibits a very high activity. As the cost of cobalt is significantly lower than that of Ru, it can provide a competitive alternative to Ru in terms of cost. However, a comprehensive study on the stability is required.

## 7. Nickel-Based Catalysts

Although identified as a metal with activity toward ammonia synthesis, Ni was quickly sidelined due to a much lower activity than Fe despite Ni having a higher cost. However, new reports have highlighted new improved activity toward ammonia synthesis with Ni-based catalysts.<sup>[76,79,80,134-136]</sup> These catalysts use specifically designed support materials to interact with the Ni catalyst to achieve excellent activities, acting as cocatalysts with the Ni.

Excellent activity at low temperature and atmospheric pressure was obtained for a Ni catalyst supported on LaN by Ye et al.<sup>[134]</sup> Weakening the nitrogen triple bond through nitrogen vacancies on the LaN surface allowed for a high activity to be achieved for the Ni catalyst, overcoming its low binding energy. Activities of 2665 and 5500 μmol g<sup>-1</sup> h<sup>-1</sup> were achieved at 340 and 400 °C, respectively (0.1 MPa, 36 000 mL g<sup>-1</sup> h<sup>-1</sup>).<sup>[134]</sup> When they investigated Ni with support materials that had previously displayed excellent activity with Ru, a similar high activity was not reported with Ni. Therefore, counter to the conventional consensus that Ni-based ammonia catalysts have limited activity, it has been demonstrated that excellent activity at low temperature is obtainable.<sup>[134]</sup> However, the synergistic effect toward the support material must be fully realized to obtain this activity with carefully designed materials used to overcome the low binding energy of Ni. By utilizing the support material to weaken the nitrogen triple bond, this new class of Ni catalyst will be a type of cocatalyst.

As mentioned in the section on Fe catalysts, the chemical looping process has been shown to drastically increase the activity of hydride-supported catalysts by Gao et al.<sup>[79]</sup> As shown in the **Table 5**, an activity increase of nearly two orders of magnitude from 48 to 3125 μmol g<sup>-1</sup> h<sup>-1</sup> was observed for Ni-BaH<sub>2</sub> when switched from the conventional synthesis with a feed gas ratio of 3/1 H<sub>2</sub>/N<sub>2</sub> to the chemical looping process (300 °C, 0.1 MPa, 60 000 mL g<sup>-1</sup> h<sup>-1</sup>).<sup>[79]</sup> As was highlighted in the Fe section,

**Table 4.** Chemical composition and activity of selected cobalt catalysts for ammonia synthesis.

Catalyst	Promoter [wt%]	Reactor temperature [°C]	Reactor pressure [MPa]	WHSV [mL g <sup>-1</sup> h <sup>-1</sup> ]	NH <sub>3</sub> percentage in reactor outlet [v/v%]	NH <sub>3</sub> synthesis rate [μmol g <sup>-1</sup> h <sup>-1</sup> ]	Ref.
20% Co–BaH <sub>2</sub> (chemical looping process)	–	300	0.1	6000	–	1866	[79]
20% Co–BaH <sub>2</sub>	–	350	0.1	6000	–	576	[79]
CoRe <sub>4</sub>	–	400	0.1	12 000	–	943	[132]
Co <sub>3</sub> Mo <sub>3</sub> N	–	400	0.1	9000	–	652	[146]
2.6 wt% Co/C12A7:e <sup>-1</sup>	–	400	0.1	18 000	–	1764	[197]
Co <sub>3</sub> Mo <sub>3</sub> C	–	500	0.1	12 000	–	461	[198]
4.7%Co/BaCeO <sub>3-x</sub> H <sub>y</sub> N <sub>z</sub>	–	400	0.9	36 000	–	10 100	[82]
5.2 wt% Co/CNT	BaH <sub>x</sub> (Ba: 20.1 wt%)	300	1	6000	–	4800	[199]
3.4 wt% Co–N–C	–	350	1	60 000	–	4340	[200]
Co/C	0.87 Ba/Co atomic ratio	400	1	–	–	43 200	[122]
Co/CeO <sub>2</sub> -D-500	–	425	1	–	–	19 120	[201]
CoPc	8% Ba	400	3	12 000	–	10 250	[155]
CoRe <sub>4</sub>	–	350	3.1	9000	–	2400	[202]
1%Co/BaTiO <sub>3-x</sub> H <sub>x</sub>	–	400	5	66 000	–	5700	[81]
Co	11.5 wt% CeO <sub>2</sub> , Ba	400	6.3	175 000	–	195 880	[127]
Co	0.6 mmol g <sub>(C+Co)</sub> <sup>-1</sup> Ba	400	6.3	175 000	0.7	52 352	[125]
Co	0.52 mmol g <sub>(C+Co)</sub> <sup>-1</sup> Ce	400	6.3	175 000	0.07	4705	[125]
Co	0.52 mmol g <sub>(C+Co)</sub> <sup>-1</sup> Ce, 1.17 mmol g <sub>(C+Co)</sub> <sup>-1</sup> Ba	400	6.3	175 000	1.7	116 470	[125]
Co/Ba(CP)	Ba (2 wt%)	400	6.3	70 000	–	70 905	[203]
Co	1.2 mmol g <sup>-1</sup> (Co) Ba	430	6.3	233 333	–	1666	[133]
Co	7.4 wt% La	430	6.3	233 333	–	103 333	[133]
Co	1.4 mmol g <sup>-1</sup> (Co) Ba, 7.4 wt% La	430	6.3	233 333	–	181666	[133]
Co	0.88 mmol g <sub>(C+Co)</sub> <sup>-1</sup> Ba	430	6.3	175 000	–	–	[126]
Co	0.75 mmol g <sub>(C+Co)</sub> <sup>-1</sup> Ce	430	6.3	175 000	–	–	[126]
Co	0.75 mmol g <sub>(C+Co)</sub> <sup>-1</sup> Ce, 1.02 mmol g <sub>(C+Co)</sub> <sup>-1</sup> Ba	430	6.3	175 000	–	–	[126]
8.4% Co/Mg–La	–	470	6.3	140 000	–	54 000	[204]
Co/C	0.69 mmol g <sub>(C+Co)</sub> <sup>-1</sup> Ba	400	9	70 000	–	83 333	[131]
26.8%Co/C	Ba	400	9	144 444	–	84 444	[124]
(Co–Ce) <sub>1</sub> /C	0.071 mmol g <sub>(C+Co)</sub> <sup>-1</sup> Ce, 0.89 mmol g <sub>(C+Co)</sub> <sup>-1</sup> Ba	400	9	155 555	–	452 390	[128]
(Co–Ce) <sub>5</sub> /C	0.074 mmol g <sub>(C+Co)</sub> <sup>-1</sup> Ce, 0.89 mmol g <sub>(C+Co)</sub> <sup>-1</sup> Ba	400	9	155 555	–	294 283	[128]
Co <sub>R</sub> /C	0.84 mmol g <sub>(C+Co)</sub> <sup>-1</sup> Ba	470	9	14 444	–	99 411	[123]
Co <sub>R+P</sub> /C	0.92 mmol g <sub>(C+Co)</sub> <sup>-1</sup> Ba	470	9	14 444	–	18 823	[123]
Co <sub>R+P+C</sub> /C	0.73 mmol g <sub>(C+Co)</sub> <sup>-1</sup> Ba	470	9	14 444	–	127 647	[123]
Co/CeO <sub>2</sub>	–	430	10	240 000	–	52 040	[129]
6 wt% Co/CeO <sub>2</sub>	Ba (3 wt%)	430	10	–	–	26 654	[205]
10 wt% Co/CeO <sub>2</sub>	–	430	10	–	–	86 000	[206]

the chemical looping process elevates the Ni catalyst above the Fe one despite lower activities in the conventional synthesis process. During the chemical looping process, nitridation of the BaH<sub>2</sub> support takes place, forming BaNH during the nitrogen loop. When looking at the conclusions from Ye et al.,<sup>[134]</sup> where it is noted that high Ni activity relies on the breaking of the

nitrogen triple bond to overcome the low binding energy of Ni, this favorable performance of the chemical looping process with Ni catalysts makes sense. If the nitrogen triple bond in N<sub>2</sub> is broken on the BaH<sub>2</sub> to form BaNH then this will also act as a co-catalyst to the Ni, overcoming its weakness. Table 5 shows the activity of a range of nickel-based catalysts for ammonia synthesis.



**Table 5.** Chemical composition and activity of selected nickel catalysts for ammonia synthesis.

Catalyst	Ni loading [wt%]	Reactor temperature [°C]	Reactor pressure [MPa]	WHSV [mL g <sup>-1</sup> h <sup>-1</sup> ]	NH <sub>3</sub> percentage in reactor outlet [v/v%]	NH <sub>3</sub> synthesis rate [μmol g <sup>-1</sup> h <sup>-1</sup> ]	Ref.
Ni–BaH <sub>2</sub>	20	300	0.1	60 000	–	48	[79]
Ni–BaH <sub>2</sub> (chemical looping)	50	300	0.1	60 000	–	3125	[79]
Ni–LiH	59.5	300	0.1	60 000	–	40	[76]
Ni–LiH (chemical looping)	50	300	0.1	60 000	–	1533	[79]
Ni/LaN NPs	12.5	340	0.1	36 000	–	2665	[134]
Ni/LaN bulk	5	340	0.1	36 000	–	820	[134]
Ni–Mo–N	34.8	400	0.1	9000	–	275	[135]
Ni <sub>2</sub> Mo <sub>3</sub> N	28	400	0.1	9000	–	395	[136]
Ni–BaZr <sub>0.1</sub> Ce <sub>0.7</sub> Y <sub>0.2</sub> O <sub>3–δ</sub>	54	620	0.1	30 000	–	250	[80]
Ni/CeN NPs	11.7	400	0.9	36 000	–	6500	[150]

Low-temperature ammonia synthesis remains one of the key challenges facing catalysts today, with the commonly used fused-Fe catalysts not able to reach the low temperatures achieved by the expensive ruthenium catalysts. However, these low temperatures can be reached by Ni catalysts, as shown in the table, with good activities for temperatures as low as 300 °C reported. Industrially, fused-Fe catalysts are still used over Ru catalysts due to the greatly reduced cost. However, despite still costing more than Fe, these Ni catalysts are much cheaper than Ru and therefore may provide cost-effective catalysts for low-temperature and pressure ammonia synthesis plants.

## 8. Metal Nitride Catalysts

In addition to the metal (Fe, Ru, Co)-based catalysts, a number of metal nitride phases have also been reported for their high activity in the catalytic synthesis of ammonia. Binary nitride systems based on uranium,<sup>[137]</sup> cerium,<sup>[138]</sup> vanadium,<sup>[139]</sup> molybdenum,<sup>[140]</sup> and rhenium<sup>[141]</sup> have been reported over the last century with the catalytic activity of uranium nitrate reported by Haber.<sup>[142]</sup>

One major development in metal nitride catalysts was the idea of ternary nitride systems.<sup>[2,143,144]</sup> This idea can be shown by looking at the volcano-type plot obtained for the DFT-calculated turnover frequencies of various ammonia synthesis catalysts.<sup>[144]</sup> These turnover frequency values were calculated through a combination of a microkinetic model for the synthesis rate and the linear relation that exists for the N<sub>2</sub> dissociation potential energy and activation energy. Their model also accounts for potassium and cesium promoters. This plot is shown in **Figure 10**.

It can be seen that if a ternary nitride is made by combining two metals, one with too high a nitrogen adsorption energy and one with a nitrogen adsorption energy that is too low, then an ammonia synthesis catalyst can be obtained with a TOF closer to the maximum than any single metal nitride.<sup>[2,144]</sup> In the Co–Mo catalyst system shown on the plot, Mo binds nitrogen too strongly,<sup>[2]</sup> whereas Co binds nitrogen too weakly.<sup>[2]</sup> These results were confirmed experimentally in a study by Jacobsen et al.<sup>[145]</sup> in which the ternary nitride catalysts Fe<sub>3</sub>Mo<sub>3</sub>N, Co<sub>3</sub>Mo<sub>3</sub>N, and Ni<sub>2</sub>Mo<sub>3</sub>N were tested with promoters. They

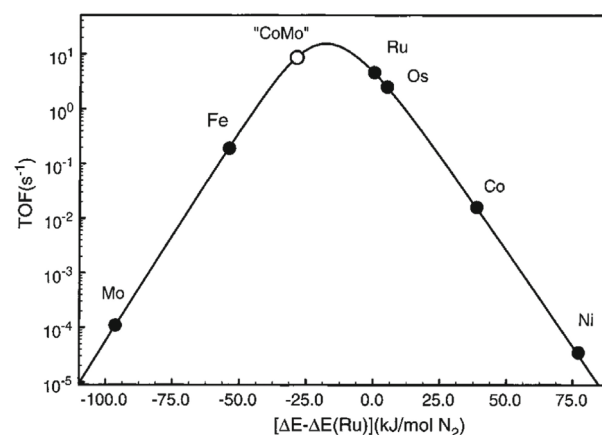


**Figure 10.** Calculated turnover frequencies for ammonia synthesis as a function of nitrogen adsorption energy (400 °C, 50 bar). Reproduced with permission.<sup>[144]</sup> Copyright 2001, American chemical society.

obtained these nitrides by mixing a solution of metal nitrate salt required for the system with a solution of ammonium heptamolybdate which was dried and calcined at 400 °C for 2 h. This produced MMoO<sub>4</sub>·xH<sub>2</sub>O (where M = Fe, Co, Ni), which was heated to 600 °C in 4.5% ammonia and 3:1 H<sub>2</sub>–N<sub>2</sub>.<sup>[145]</sup> They used cesium nitrate as the catalyst promoter through impregnation of the oxide either before ammonolysis or directly on to the catalyst.<sup>[145]</sup>

The role of the preparation method on the activity of the Ni<sub>2</sub>Mo<sub>3</sub>N catalyst was investigated by Bion et al. in 2014.<sup>[136]</sup> To investigate the preparation method, two different preparation routes were applied; these were the nitridation of NiMoO<sub>4</sub> and the second was the nitridation of a mixed phase precursor formed through the Pechani method. In their results they reported an ammonia synthesis rate of less than 15 μmol h<sup>-1</sup> g<sup>-1</sup> for the catalyst prepared through the nitridation of NiMoO<sub>4</sub>; however, for the catalyst prepared using the Pechani method the rate increased to 395 μmol h<sup>-1</sup> g<sup>-1</sup> under the same conditions of ambient pressure and 400 °C.<sup>[136]</sup> This was due to the presence of a large amount of Ni impurities in the catalyst formed from the nitridation of NiMoO<sub>4</sub>.<sup>[136]</sup>

In 2001, Kojima and Aika<sup>[146]</sup> investigated the preparation method for  $\text{Co}_3\text{Mo}_3\text{N}$  catalysts and its effect on activity for ammonia synthesis. In their preparation they used cobalt molybdate hydrate as the precursor. This precursor was prepared by the addition of  $\text{Co}(\text{NO}_3)_2 \cdot 6\text{H}_2\text{O}$  to a heated ammonium molybdate solution.<sup>[146]</sup> Nitrates of potassium and cesium were used as promoters and were added to the cobalt molybdate hydrate precursor through impregnation. The nitridation of the cobalt molybdate hydrate precursor was then achieved using flowing ammonia in a temperature-programmed quartz reactor. The heating program involved heating to 973 K at a rate of  $5 \text{ K min}^{-1}$  with the 973 K maintained for 6 h before quenching to room temperature.<sup>[146]</sup> The activity of the catalyst was then tested at 673 K at 0.1 MPa using a gas flow rate of  $45 \text{ mL min}^{-1} \text{ H}_2$  and  $15 \text{ mL min}^{-1} \text{ N}_2$ . In their results they reported a rate of  $652 \mu\text{mol h}^{-1} \text{ g}^{-1}$  for the unpromoted  $\text{Co}_3\text{Mo}_3\text{N}$  catalyst.<sup>[146]</sup> This rate was shown to increase to  $869 \mu\text{mol h}^{-1} \text{ g}^{-1}$  when the catalyst was promoted with potassium with a K/Co mole ratio of 0.05. The highest rate achieved was for the cesium-promoted catalyst, which had a rate of  $986 \mu\text{mol h}^{-1} \text{ g}^{-1}$  when promoted with cesium with a Cs/Co mole ratio of 0.02.<sup>[146]</sup>

Kojima et al.<sup>[135,147]</sup> further studied the  $\text{Co}_3\text{Mo}_3\text{N}$  catalyst, finding that the main adsorption species was  $\text{NH}_2$  on the non-promoted catalyst, with it changing to  $\text{NH}$  for the alkali-promoted one. They also investigated the nitridation conditions, finding that a poorly crystalline phase forms when heated to 673 K under ammonia flow. The complete  $\text{Co}_3\text{Mo}_3\text{N}$  phase was found when heated at either 973 K for 3 h or 873 K for 12 h.

In 2008, McKay et al.<sup>[148]</sup> synthesized the  $\text{Co}_3\text{Mo}_3\text{N}$  catalyst along with  $\text{Fe}_3\text{Mo}_3\text{N}$ ,  $\text{Ni}_2\text{Mo}_3\text{N}$ ,  $\gamma\text{-Mo}_2\text{N}$ ,  $\beta\text{-Mo}_2\text{N}_{0.78}$ , and  $\delta\text{-MoN}$  to investigate their activity as ammonia synthesis catalysts. To prepare  $\gamma\text{-Mo}_2\text{N}$ , they conducted nitridation using ammonia gas with a  $\text{MoO}_3$  precursor. To synthesize the  $\beta\text{-Mo}_2\text{N}_{0.78}$  catalyst, they flew nitrogen and hydrogen with a  $\text{H}_2/\text{N}_2$  mole ratio of 3/1 over the  $\text{MoO}_3$  precursor in situ in the microreactor.  $\text{MoN}$  was synthesized through the nitridation of  $\text{MoS}_2$  with ammonia gas. To prepare  $\text{Co}_3\text{Mo}_3\text{N}$ ,  $\text{Fe}_3\text{Mo}_3\text{N}$ , and  $\text{Ni}_2\text{Mo}_3\text{N}$ , the metal nitrate of either Co, Fe, or Ni was mixed with an ammonium molybdate solution, dried, and then nitridated following the same procedure as that for  $\gamma\text{-Mo}_2\text{N}$ . They conducted their activity measurements at 0.1 MPa,  $400^\circ\text{C}$ , and using a  $\text{H}_2/\text{N}_2$  mole ratio of 3/1, with an overall flow rate of  $60 \text{ mL min}^{-1}$ . Their results are reported in Table 6,<sup>[148]</sup> where it can be seen that their activity for the  $\text{Co}_3\text{Mo}_3\text{N}$  catalyst is significantly lower than that reported by Kojima and Aika.<sup>[146]</sup>

Alongside the ternary nitrides that are highlighted in Table 6, Cao et al.<sup>[149]</sup> have reported on ternary amides of transition and alkali metals. Both  $\text{Rb}_2[\text{Mn}(\text{NH}_2)_4]$  and  $\text{K}_2[\text{Mn}(\text{NH}_2)_4]$  were synthesized through ball milling the respective metals at room temperature under 0.7 MPa of  $\text{NH}_3$ . They both exhibited a significant activity increase over the best performing ternary nitride catalyst, which was  $\text{Co}_3\text{Mo}_3\text{N}$ , with activities of  $11 \text{ mmol g}^{-1} \text{ h}^{-1}$  for  $\text{K}_2[\text{Mn}(\text{NH}_2)_4]$ ,  $6 \text{ mmol g}^{-1} \text{ h}^{-1}$  for  $\text{Rb}_2[\text{Mn}(\text{NH}_2)_4]$ , and  $5.3 \text{ mmol g}^{-1} \text{ h}^{-1}$  for  $\text{Co}_3\text{Mo}_3\text{N}$ , all of which were measured at  $400^\circ\text{C}$  and 1 MPa.<sup>[145,149]</sup> This increase in activity was also reported at a much-reduced pressure, with the ternary amides tested at 1 MPa compared to 10 MPa for  $\text{Co}_3\text{Mo}_3\text{N}$ . Along with the results highlighted in the previous section where an increase in activity is noted when the support material for a Ru catalyst is

changed from hydride to amide ( $\text{CaH}_2$  to  $\text{Ca}(\text{NH}_2)_2$ ),<sup>[105,116]</sup> this move from ternary nitrides to ternary amides may be the key next step in this class of catalysts.

Nitrogen vacancies in these nitride catalysts have been investigated in a study by Ye et al.<sup>[134]</sup> in which a Ni-LaN catalyst was used. An activity of  $5500 \text{ mmol g}^{-1} \text{ h}^{-1}$  was reported at a temperature of  $400^\circ\text{C}$  and atmospheric pressure. They reported that surface nitrogen vacancies in LaN weakened the N triple bond, and the  $\text{H}_2$  dissociation on the Ni surface also contributed to this. Due to its low binding energy for  $\text{N}_2$ , Ni is not as commonly reported as other more conventional ammonia synthesis catalysts such as Ru and Fe. The poor performance of Ni was shown by Ye et al.<sup>[134]</sup> when Ni was used with excellent Ru supports such as C12A7:e<sup>-1</sup> and MgO. However, due to the weakening of the N triple bond through nitrogen vacancies on the LaN surface, this weakness of the Ni catalyst can be overcome with activities in line with those of much more expensive Ru catalysts.

Ye et al. furthered their work in this area with Ni-CeN, gaining a better insight into the nature of the ammonia synthesis reaction on this new catalyst class.<sup>[150]</sup> An activity of  $6500 \mu\text{mol g}^{-1} \text{ h}^{-1}$  was achieved for Ni-CeN at  $400^\circ\text{C}$ , 0.9 MPa, and a WHSV of  $36\,000 \text{ mL g}^{-1} \text{ h}^{-1}$ .<sup>[150]</sup> The nitrogen vacancies generated in the metal nitride, CeN, were responsible for the activation of  $\text{N}_2$  in the catalyst system and the Ni in this system was responsible for  $\text{H}_2$  activation. This changes the system for the conventional catalyst and promoter to a cocatalyst system where each part performs its own task in ammonia synthesis. The strong hydrogen adsorption energy of Ni compared to the nitrogen vacancies in the cocatalyst, calculated as  $-1.30$  and  $-0.62 \text{ eV}$ , respectively, by Ye et al. enables the dissociate hydrogen adsorption step to take place preferentially on the Ni catalyst.<sup>[150]</sup> Ammonia is produced from the reaction of adsorbed hydrogen and lattice nitrogen in the CeN catalyst; the produced vacant nitrogen sites resulting from this are then used in the nitrogen gas activation step, thereby achieving continuous ammonia synthesis.<sup>[150]</sup> The mechanism proposed for this was further investigated through nitrogen isotope experiments in which ammonia synthesis was conducted with  $^{15}\text{N}_2$  and  $\text{H}_2$  using the pure CeN catalyst.<sup>[150]</sup> This provided further confirmation that lattice nitrogen ( $^{14}\text{N}$ ) in CeN takes place in the ammonia synthesis reaction. To further understand the activity of these catalysts, DFT calculations were performed with the nitrogen vacancy formation energy calculated. In their calculations they found that the nitrogen vacancy formation energy was lowest for Ni-CeN, further increasing for Ni-LaN, Ni-YN, and finally Ni-ScN with the highest nitrogen vacancy formation energy.<sup>[150]</sup>

The reported catalytic activities for nitride-based catalysts are listed in Table 6. The Cs- or K-promoted  $\text{Co}_3\text{Mo}_3\text{N}$  catalysts exhibit a high activity of  $\approx 900 \mu\text{mol g}^{-1} \text{ h}^{-1}$  at  $400^\circ\text{C}$  and 1 bar, which is comparable to Fe- and Co-based catalysts under the same condition.<sup>[66,146]</sup> However, the cost of these nitride catalysts is much higher than that for fused-Fe catalysts, which is the major barrier for large-scale applications. Further investigation of the activity under high pressure and the stability of nitrides in the presence of oxygenates such as  $\text{O}_2$ ,  $\text{H}_2\text{O}$ , and CO at high temperature is required to fully understand their potential as real industrial ammonia synthesis catalysts. At high temperature, nitrides tend to be oxidized to oxynitrides or oxides in the presence of oxygenates.<sup>[151]</sup> The effect of this oxidation

**Table 6.** Catalytic ammonia synthesis activities of molybdenum nitride and ternary nitrides.

Catalyst	Promoter [wt%]	Reactor temperature [°C]	Reactor pressure [MPa]	WHSV [mL g <sup>-1</sup> h <sup>-1</sup> ]	NH <sub>3</sub> synthesis rate [mL h <sup>-1</sup> g <sup>-1</sup> ]	NH <sub>3</sub> synthesis rate [μmol g <sup>-1</sup> h <sup>-1</sup> ]	Ref.
γ-Mo <sub>2</sub> N	–	400	0.1	9000	–	34	[148]
β-Mo <sub>2</sub> N <sub>0.78</sub>	–	400	0.1	9000	–	35	[148]
δ-MoN	–	400	0.1	9000	–	4	[148]
Co <sub>3</sub> Mo <sub>3</sub> N	–	400	0.1	9000	–	167	[148]
Co <sub>3</sub> Mo <sub>3</sub> N	–	400	0.1	9000	–	652	[146]
Fe <sub>3</sub> Mo <sub>3</sub> N	–	400	0.1	9000	–	95	[148]
Ni <sub>2</sub> Mo <sub>3</sub> N	–	400	0.1	9000	–	29	[148]
Ni <sub>2</sub> Mo <sub>3</sub> N	–	400	0.1	9000	–	395	[136]
Co <sub>3</sub> Mo <sub>3</sub> N	Cs 0.02 mol mol <sup>-1</sup> Co	400	0.1	9000	–	869	[146]
Co <sub>3</sub> Mo <sub>3</sub> N	K 0.05 mol mol <sup>-1</sup> Co	400	0.1	9000	–	986	[146]
NiCoMo <sub>3</sub> N	–	400	0.1	12 000	–	166	[207]
Ni–LaN	–	400	0.1	36 000	–	5543	[134]
Ni <sub>1.1</sub> Fe <sub>0.9</sub> Mo <sub>3</sub> N	–	500	0.1	5200	–	354	[208]
CeN NPs	–	400	0.9	36 000	–	1450	[150]
K <sub>2</sub> [Mn(NH <sub>2</sub> ) <sub>4</sub> ]	–	400	1	6000	–	11 141	[149]
γ-Mo <sub>2</sub> N	–	400	10	–	30	–	[145]
Co <sub>3</sub> Mo <sub>3</sub> N	–	400	10	–	120	–	[145]
Fe <sub>3</sub> Mo <sub>3</sub> N	–	400	10	–	90	–	[145]
Ni <sub>2</sub> Mo <sub>3</sub> N	–	400	10	–	80	–	[145]
Co <sub>3</sub> Mo <sub>3</sub> N	Cs (5 wt%)	400	10	–	1040	–	[145]
Fe <sub>3</sub> Mo <sub>3</sub> N	Cs (5 wt%)	400	10	–	440	–	[145]
Ni <sub>2</sub> Mo <sub>3</sub> N	Cs (5 wt%)	400	10	–	530	–	[145]

process and the end products on the activity of ammonia synthesis should be investigated to fully understand the potential of nitride-based catalysts. In terms of stability in oxygenates, the oxide-based promoter/cocatalyst, functionalized by oxygen vacancies, such as Ce<sub>0.8</sub>Sm<sub>0.2</sub>O<sub>2-δ</sub>, is a better option.<sup>[84]</sup>

## 9. Conclusion

Through the last 100 years of development, the catalytic synthesis of ammonia appears to have become a mature technology. However, there is still a large volume of recent publications on the development of ammonia synthesis catalysts for the conventional Haber–Bosch process using a wide range of catalysts such as promoted-iron catalysts, supported ruthenium catalysts, and metal nitride catalysts. Although current research is now focusing on the development of new highly active ammonia synthesis catalysts using ruthenium, cobalt, nickel, and metal nitrides, the lessons learned from the extensive study of the promoted-iron catalyst, from its initial discovery to its widespread global use on an industrial scale, will help us improve the Haber–Bosch process through increased conversion by operating at reduced temperature and pressure. The new emerging ammonia synthesis catalysts such as those using electrides, hydrides, amides, nitrides, oxynitride hydride and oxide support materials are promising alternatives to the conventional Ru- and Fe-based

catalysts, but also to Ni- and Co-based catalysts. The effect of the catalyst and the support morphology has also been emphasized over the years to show that even when promising catalysts are discovered, there is still much that can be done to further increase activity. Anion vacancies, particularly oxygen and nitrogen vacancies, in promoters/cocatalysts play important roles in improving both the activity and stability of ammonia synthesis catalysts. To enable the Haber–Bosch process for localized small-scale green ammonia production, it is desirable to develop oxygenate-tolerant catalysts to simplify the gas purification process, improving the overall efficiency. A comprehensive stability study under different operating conditions with the presence of various impurities in the precursor gases is required to validate these new catalysts for industrial applications. To make the new catalysts competitive with the cheap fused-Fe catalysts, cost is an important aspect to be considered. The benefits from improved catalytic activity should not be lost through a large catalyst cost if the goal of replacing existing fused-Fe catalysts is to be achieved. As such, the key challenges facing ammonia synthesis today are outlined subsequently. 1) Although ammonia synthesis is exothermic and can achieve higher thermodynamic conversions at lower temperatures, catalysts currently require elevated temperatures to achieve a viable rate. Future catalysts should be designed to operate at as low a temperature as possible to maximize conversion per reactor loop. New Ni-based catalysts supported on LaN have been shown to provide activity at low

Received: September 25, 2020

Revised: November 5, 2020

Published online:

temperatures, along with Ni catalysts supported on hydrides using the chemical looping process. Therefore, it is expected that Ni catalysts with specifically designed support materials may provide the key to low-temperature ammonia synthesis. Ru supported on CaFH achieved ammonia synthesis at an exceptionally low temperature of 50 °C, with weak ionic bonds in the solid solution attributed to the activity at this low temperature, again providing a key area for future research. 2) Oxygenates in the feed gas stream poison ammonia synthesis catalysts, greatly reducing their activity. Therefore, extensive purification processes are currently used in ammonia synthesis plants. These purification processes not only increase the initial and operating costs of large-scale ammonia synthesis plants but limit small-scale green ammonia synthesis, making such processes unfeasible. The doped-oxide support material  $Ce_{0.8}Sm_{0.2}O_{2-\delta}$  was shown to provide excellent tolerance for Fe toward oxygenates when used as a promoter. This promotion effect was attributed to oxygen vacancies and the SMSI effect leading to enhanced oxygenate tolerance over fused-iron industrial catalysts. When injecting 150 ppm of  $O_2$  into the feed gas stream, the  $Ce_{0.8}Sm_{0.2}O_{2-\delta}$ -promoted catalyst retained 47.4% of its activity, whereas the commercial wüstite and magnetite only retained 26.4% and 7.6%, respectively. Therefore, catalyst promoters that exhibit oxygen and anion vacancies as well as enabling the SMSI effect may pave the way for oxygenate-tolerant ammonia synthesis catalysts. 3) When designing new catalysts to address the aforementioned major challenges, it is important to consider catalyst cost. Despite the numerous highly active catalysts reported, fused-iron catalysts still make up the vast majority of catalysts used in ammonia synthesis plants due to their cost. Support and promoter materials have been shown to enable low-temperature synthesis and oxygenate tolerance, but expensive precursors and synthesis methods will limit their application to real processes. These expensive promoters are commonly used in a large weight percentage as support materials, even when the expensive Ru catalyst is replaced with the cheaper Fe one. The  $Ce_{0.8}Sm_{0.2}O_{2-\delta}$  promoter only makes up 20 wt% of the catalyst, with the remaining 80 wt% made up by Fe, close to the Fe content in the fused-iron catalyst ( $\approx 90$  wt%).

Moving forward, addressing these challenges will be key to improving and evolving ammonia production, not only in the current large-scale production but also in opening the door toward small-scale localized green ammonia production using low-carbon renewable energy sources.

## Acknowledgements

The authors thank the EPSRC for the funding (Grant No EP/G01244X/1).

## Conflict of Interest

The authors declare no conflict of interest.

## Keywords

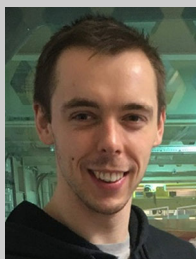
catalysts, green ammonia, Haber–Bosch process, oxygenate tolerance

- [1] J. W. Erisman, M. A. Sutton, J. Galloway, Z. Klimont, W. Winiwarter, *Nat. Geosci.* **2008**, *1*, 636.
- [2] H. Liu, *Ammonia Synthesis Catalysts Innovation and Practice*, Vol. 1, World Scientific Publishing Co/Chemical Industry Press, Singapore/Beijing **2013**, p. 871.
- [3] H. Liu, *Chin. J. Catal.* **2014**, *35*, 1619.
- [4] R. Lan, J. T. S. Irvine, S. W. Tao, *Int. J. Hydrogen Energy* **2012**, *37*, 1482.
- [5] D. R. MacFarlane, P. V. Cherepanov, J. Choi, B. H. Suryanto, R. Y. Hodgetts, J. M. Bakker, F. M. Vallana, A. N. Simonov, *Joule* **2020**, *4*, 1186.
- [6] R. M. Nayak-Luke, R. Bañares-Alcántara, *Energy Environ. Sci.* **2020**, *13*, 2957.
- [7] M. Kitano, Y. Inoue, Y. Yamazaki, F. Hayashi, S. Kanbara, S. Matsuishi, T. Yokoyama, S. W. Kim, M. Hara, H. Hosono, *Nat. Chem.* **2012**, *4*, 934.
- [8] C. Smith, A. K. Hill, L. Torrente-Murciano, *Energy Environ. Sci.* **2020**, *13*, 331.
- [9] S. Giddey, S. P. S. Badwal, A. Kulkarni, *Int. J. Hydrogen Energy* **2013**, *38*, 14576.
- [10] W. Weiss, W. Ranke, *Prog. Surf. Sci.* **2002**, *70*, 1.
- [11] J. R. Jennings, *Catalytic Ammonia Synthesis: Fundamentals and Practice*, Springer Science & Business Media, New York **2013**.
- [12] N. Saadatjou, A. Jafari, S. Sahebdehfar, *Chem. Eng. Commun.* **2015**, *202*, 420.
- [13] M. Neurock, *AIChE J.* **1994**, *40*, 1085.
- [14] P. Stoltze, J. K. Norskov, *J. Catal.* **1988**, *110*, 1.
- [15] M. Bowker, I. B. Parker, K. C. Waugh, *Appl. Catal.* **1985**, *14*, 101.
- [16] P. Stoltze, J. K. Norskov, *Phys. Rev. Lett.* **1985**, *55*, 2502.
- [17] G. Ertl, *Catal. Rev. Sci. Eng.* **1980**, *21*, 201.
- [18] M. S. Spencer, *Catal. Lett.* **1992**, *13*, 45.
- [19] H. D. Vandervell, K. C. Waugh, *Chem. Phys. Lett.* **1990**, *171*, 462.
- [20] P. H. Emmett, S. Brunauer, *J. Am. Chem. Soc.* **1934**, *56*, 35.
- [21] F. Bozso, G. Ertl, M. Grunze, M. Weiss, *J. Catal.* **1977**, *49*, 18.
- [22] F. Bozso, G. Ertl, M. Weiss, *J. Catal.* **1977**, *50*, 519.
- [23] G. Ertl, M. Weiss, S. B. Lee, *Chem. Phys. Lett.* **1979**, *60*, 391.
- [24] G. Ertl, S. B. Lee, M. Weiss, *Surf. Sci.* **1982**, *114*, 527.
- [25] C. T. Rettner, H. Stein, *Phys. Rev. Lett.* **1987**, *59*, 2768.
- [26] J. J. Scholten, P. Zwietering, J. A. Konvalinka, J. H. De Boer, *Trans. Faraday Soc.* **1959**, *55*, 2166.
- [27] D. W. Johnson, M. W. Roberts, *Surf. Sci.* **1979**, *87*, L255.
- [28] F. Haber, *Nobel Lecture 1920*.
- [29] M. Appl, in *Ullmann's Encyclopedia of Industrial Chemistry*, Wiley-VCH Verlag GmbH & Co. KGaA, Weinheim **2011**, pp. 139–210.
- [30] L. J. Gillespie, J. A. Beattie, *Phys. Rev.* **1930**, *36*, 743.
- [31] O. Stepan, B. Stverak, *Collect. Czech. Chem. Commun.* **1971**, *36*, 2358.
- [32] M. Boudart, S. B. Khammoum, *Abstr. Pap. Am. Chem. Soc.* **1972**, *164*, 15.
- [33] D. Zubritsk, Y. Lyubchen, K. Mikhalev, V. Litvinch, R. Chesnoko, K. D. Konkov, V. V. Dovgei, *Zhurnal Prikladnoi Khimii* **1973**, *46*, 329.
- [34] M. G. Berengar, L. A. Rudnitskij, P. D. Rabina, L. D. Kuznetsov, I. E. Zubova, A. M. Alekseev, K. Z. Zakieva, *Dokl. Akad. Nauk SSSR* **1974**, *214*, 601.
- [35] V. S. Badik, Y. A. Lyubchenko, A. N. Sergeeva, L. M. Dmitrenko, *J. Appl. Chem.* **1974**, *47*, 2239.
- [36] O. S. Dvornik, O. A. Streltsov, Y. A. Lyubchenko, *Dokl. Akad. Nauk SSSR* **1975**, *221*, 648.
- [37] Y. M. Artyukh, R. Bondarenko, V. Golovatii, G. Kozub, *Dopov. Akad. Nauk. B* **1975**, 121.
- [38] V. N. Anokhin, V. N. Menshov, A. A. Zuev, *J. Appl. Chem.* **1975**, *48*, 509.

- [39] O. S. Dvornik, O. A. Streltsov, V. L. Chernobrivets, *Ukr. Khim. Zh.* **1975**, *41*, 544.
- [40] V. Y. Zabuga, M. V. Tovbin, L. A. Chernysheva, I. I. Drel, N. I. Efimova, *Ukr. Khim. Zh.* **1975**, *41*, 818.
- [41] V. K. Yatsimirskii, M. Piontkovskaya, L. Kuzmenko, M. Dubovik, I. Matyash, V. Ivanitskii, T. Kozlova, *Kinet. Catal.* **1976**, *17*, 1123.
- [42] D. C. Silverman, M. Boudart, *Society* **1977**, *174*, 50.
- [43] V. S. Komarov, A. T. Rozin, *Dokl. Akad. Nauk Belarusi* **1977**, *21*, 1102.
- [44] I. A. Simulina, N. Karibdzhanyan, S. Lachinov, V. Anfimov, Z. Shumlyakovskiy, *Khim. Prom-sti* **1977**, 119.
- [45] O. S. Dvornik, O. A. Streltsov, Y. N. Artyukh, *Ukr. Khim. Zh.* **1977**, *43*, 375.
- [46] A. Baranski, A. Pattek, A. Reizer, *Bull. Acad. Polonaise Sci.* **1978**, *26*, 353.
- [47] X. J. Yu, L. I. Bingyu, L. I. Jianxin, W. A. Rong, W. E. Kemei, *J. Rare Earths* **2008**, *26*, 711.
- [48] M. Penkuhn, G. Tsatsaronis, *Energy* **2017**, *137*, 854.
- [49] *Ammonia Synthesis, in Synthetic Nitrogen Products: A Practical Guide to the Products and Processes* (Ed: G. R. Maxwell), Springer US, Boston **2004**, pp. 163–198.
- [50] M. Malmali, Y. Wei, A. McCormick, E. L. Cussler, *Ind. Eng. Chem. Res.* **2016**, *55*, 8922.
- [51] M. Malmali, G. Le, J. Hendrickson, J. Prince, A. V. McCormick, E. L. Cussler, *ACS Sustainable Chem. Eng.* **2018**, *6*, 6536.
- [52] K. Wagner, M. Malmali, C. Smith, A. McCormick, E. L. Cussler, M. Zhu, N. C. Seaton, *AIChE J.* **2017**, *63*, 3058.
- [53] M. Malmali, M. Reese, A. V. McCormick, E. L. Cussler, *ACS Sustainable Chem. Eng.* **2018**, *6*, 827.
- [54] U. Schwertmann, R. M. Cornell, *Iron Oxides in the Laboratory: Preparation and Characterization. Xiv+137p*, Vch Verlagsgesellschaft Mbh, Weinheim, Germany, Vch Publishers, Inc., New York, NY **1991**, XIV+137P.
- [55] J. A. Almquist, E. D. Crittenden, *Ind. Eng. Chem.* **1926**, *18*, 1307.
- [56] G. L. Bridger, G. R. Pole, A. W. Beinlich, H. L. Thompson, *Chem. Eng. Progress* **1947**, *43*, 291.
- [57] K.-I. Aika, A. Ozaki, *J. Catal.* **1970**, *19*, 350.
- [58] K.-I. Aika, A. Ozaki, *J. Catal.* **1969**, *13*, 232.
- [59] A. Baranski, A. Bielanski, A. Pattek, *J. Catal.* **1972**, *26*, 286.
- [60] J. A. Dumesic, H. Topsøe, S. Khammouma, M. Boudart, *J. Catal.* **1975**, *37*, 503.
- [61] J. G. V. Ommen, W. J. Bolink, J. Prasad, P. Mars, *J. Catal.* **1975**, *38*, 120.
- [62] K. Altenburg, H. Ommen, J. G. van Ommen, P. J. Gellings, *J. Catal.* **1980**, *66*, 326.
- [63] C. Bokhoven, R. Westrik, P. Zwietering, in *Catalysis 3* (Ed: P. H. Emmett), Reinhold, New York **1955**.
- [64] S. Brunauer, P. H. Emmett, *J. Am. Chem. Soc.* **1940**, *62*, 1732.
- [65] D. W. Taylor, P. J. Smith, D. A. Dowden, C. Kembal, D. A. Whan, *Appl. Catal.* **1982**, *3*, 161.
- [66] P. J. Smith, D. W. Taylor, D. A. Dowden, C. Kembal, D. Taylor, *Appl. Catal.* **1982**, *3*, 303.
- [67] N. Homs, P. R. De La Piscina, J. L. Fierro, J. E. Sueiras, *Z. Anorg. Allg. Chem.* **1984**, *518*, 227.
- [68] S. R. Bare, D. R. Strongin, G. A. Somorjai, *J. Phys. Chem.* **1986**, *90*, 4726.
- [69] D. R. Strongin, S. R. Bare, G. A. Somorjai, *J. Catal.* **1987**, *103*, 289.
- [70] A. Baiker, R. Schlogl, E. Armbruster, H. Güntherodt, *J. Catal.* **1987**, *107*, 221.
- [71] A. Baiker, H. Baris, R. Schlögl, *J. Catal.* **1987**, *108*, 467.
- [72] R. Schlögl, R. Wiesendanger, A. Baiker, *J. Catal.* **1987**, *108*, 452.
- [73] N. D. Spencer, R. C. Schoonmaker, G. A. Somorjai, *J. Catal.* **1982**, *74*, 129.
- [74] D. R. Strongin, J. Carrazza, S. R. Bare, G. A. Somorjai, *J. Catal.* **1987**, *103*, 213.
- [75] W. Han, S. Huang, T. Cheng, H. Tang, Y. Li, H. Liu, *Appl. Surf. Sci.* **2015**, *353*, 17.
- [76] P. Wang, F. Chang, W. Gao, J. Guo, G. Wu, T. He, P. Chen, *Nat. Chem.* **2016**, *9*, 64.
- [77] Y. Ogura, K. Sato, S. I. Miyahara, Y. Kawano, T. Toriyama, T. Yamamoto, S. Matsumura, S. Hosokawa, K. Nagaoka, *Chem. Sci.* **2018**, *9*, 2230.
- [78] W. Gao, J. Guo, P. Chen, *Chin. J. Chem.* **2019**, *37*, 442.
- [79] W. Gao, J. Guo, P. Wang, Q. Wang, F. Chang, Q. Pei, W. Zhang, L. Liu, P. Chen, *Nat. Energy* **2018**, *3*, 1067.
- [80] J. Humphreys, R. Lan, D. Du, W. Xu, S. Tao, *Int. J. Hydrogen Energy* **2018**, *43*, 17726.
- [81] Y. Tang, Y. Kobayashi, N. Masuda, Y. Uchida, H. Okamoto, T. Kageyama, S. Hosokawa, F. Loyer, K. Mitsuhashi, K. Yamanaka, Y. Tamenori, *Adv. Energy Mater.* **2018**, *8*, 1801772.
- [82] M. Kitano, J. Kujirai, K. Ogasawara, S. Matsuishi, T. Tada, H. Abe, Y. Niwa, H. Hosono, *J. Am. Chem. Soc.* **2019**, *141*, 20344.
- [83] K. Murakami, Y. Tanaka, R. Sakai, K. Toko, K. Ito, A. Ishikawa, T. Higo, T. Yabe, S. Ogo, M. Ikeda, H. Tsuneki, *Catal. Today* **2020**, *351*, 119.
- [84] J. Humphreys, R. Lan, S. Chen, S. Tao, *J. Mater. Chem. A* **2020**, *8*, 16676.
- [85] B. Fastrup, H. Nygard Nielsen, *Catal. Lett.* **1992**, *14*, 233.
- [86] P. E. H. Nielsen, in *Catalytic Ammonia Synthesis Fundamentals and Practice* (Ed: J. R. Jennings), Plenum Press, New York **1991**.
- [87] J. A. Almquist, C. A. Black, *J. Am. Chem. Soc.* **1926**, *48*, 2814.
- [88] J. Folke, H. Song, J. Schittkowski, R. Schlögl, H. Ruland, *Chem. Ing. Tech.* **2020**, *92*, 1567.
- [89] C. H. Bartholomew, *Appl. Catal., A* **2001**, *212*, 17.
- [90] E. B. Maxted, *The Poisoning of Metallic Catalysts, in Advances in Catalysis* (Eds: W.G. Frankenburg, H.S. Taylor), Academic Press **1951**, pp. 129–178.
- [91] D. Xiang, *Fertilizer Catalyst Practical Manual*, Chemical Industry Press, Beijing **1992**.
- [92] J. P. Zhou, in *Proc. of the 37th American Chemical Eng. Conf. on Ammonia Plant Safety*, Shandong **1993**.
- [93] B. A. Rohr, A. R. Singh, J. K. Nørskov, *J. Catal.* **2019**, *372*, 33.
- [94] Z. Wang, J. Lin, R. Wang, K. Wei, *Catal. Commun.* **2013**, *32*, 11.
- [95] Z.-Q. Wang, Y.-C. Ma, J.-X. Lin, *J. Mol. Catal., A* **2013**, *378*, 307.
- [96] Y. Inoue, M. Kitano, S. W. Kim, T. Yokoyama, M. Hara, H. Hosono, *ACS Catal.* **2014**, *4*, 674.
- [97] H. Bielawa, O. Hinrichsen, A. Birkner, M. Muhler, *Angew. Chem., Int. Ed.* **2001**, *40*, 1061.
- [98] K. K. Chuah, S. Jaenicke, B. K. Pong, *J. Catal.* **1998**, *175*, 80.
- [99] K. Narasimharao, P. Seetharamulu, K. R. Rao, S. N. Basahel, *J. Mol. Catal., A* **2016**, *411*, 157.
- [100] B. Lin, Y. Liu, L. Heng, X. Wang, J. Ni, J. Lin, L. Jiang, *Ind. Eng. Chem. Res.* **2018**, *57*, 9127.
- [101] X. Wang, X. Peng, Y. Zhang, J. Ni, C. T. Au, L. Jiang, *Inorg. Chem. Front.* **2019**, *6*, 396.
- [102] X. Wang, X. Peng, Y. Zhang, J. Ni, C. T. Au, L. Jiang, *Ind. Eng. Chem. Res.* **2018**, *57*, 17375.
- [103] T. Ogawa, Y. Kobayashi, H. Mizoguchi, M. Kitano, H. Abe, T. Tada, Y. Toda, Y. Niwa, H. Hosono, *J. Phys. Chem. C* **2018**, *122*, 10468.
- [104] Y. Kobayashi, Y. Tang, T. Kageyama, H. Yamashita, N. Masuda, S. Hosokawa, H. Kageyama, *J. Am. Chem. Soc.* **2017**, *139*, 18240.
- [105] M. Hattori, T. Mori, T. Arai, Y. Inoue, M. Sasase, T. Tada, M. Kitano, T. Yokoyama, M. Hara, H. Hosono, *ACS Catal.* **2018**, *8*, 10977.
- [106] M. Kitano, Y. Inoue, M. Sasase, K. Kishida, Y. Kobayashi, K. Nishiyama, T. Tada, S. Kawamura, T. Yokoyama, M. Hara, H. Hosono, *Angew. Chem., Int. Ed.* **2018**, *57*, 2648.
- [107] M. Hattori, S. Iijima, T. Nakao, H. Hosono, M. Hara, *Nat. Commun.* **2020**, *11*, 2001.

- [108] C. Wildfire, V. Abdelsayed, D. Shekhawat, R. A. Dagle, S. D. Davidson, J. Hu, *Catal. Today* **2020**.
- [109] B. Lin, Y. Guo, C. Cao, J. Ni, J. Lin, L. Jiang, *Catal. Today* **2018**, 316, 230.
- [110] Ruthenium, <https://en.wikipedia.org/wiki/Ruthenium#:~:text=Ruthenium%20is%20usually%20found%20as,contacts%20and%20thick%20film%20resistors> (accessed: November 2020).
- [111] J. L. Dye, *Science* **1990**, 247, 663.
- [112] J. L. Dye, *Science* **2003**, 301, 607.
- [113] S. Matsuishi, Y. Toda, M. Miyakawa, K. Hayashi, T. Kamiya, M. Hirano, I. Tanaka, H. Hosono, *Science* **2003**, 301, 626.
- [114] M. Kitano, S. Kanbara, Y. Inoue, N. Kuganathan, P. V. Sushko, T. Yokoyama, M. Hara, H. Hosono, *Nat. Commun.* **2015**, 6, 6731.
- [115] M. Kitano, Y. Inoue, H. Ishikawa, K. Yamagata, T. Nakao, T. Tada, S. Matsuishi, T. Yokoyama, M. Hara, H. Hosono, *Chem. Sci.* **2016**, 7, 4036.
- [116] Y. Inoue, M. Kitano, K. Kishida, H. Abe, Y. Niwa, M. Sasase, Y. Fujita, H. Ishikawa, T. Yokoyama, M. Hara, H. Hosono, *ACS Catal.* **2016**, 6, 7577.
- [117] Y. Lu, J. Li, T. Tada, Y. Toda, S. Ueda, T. Yokoyama, M. Kitano, H. Hosono, *J. Am. Chem. Soc.* **2016**, 138, 3970.
- [118] Y. Lu, J. Li, T. N. Ye, Y. Kobayashi, M. Sasase, M. Kitano, H. Hosono, *ACS Catal.* **2018**, 8, 11054.
- [119] J. Wu, Y. Gong, T. Inoshita, D. C. Fredrickson, J. Wang, Y. Lu, M. Kitano, H. Hosono, *Adv. Mater.* **2017**, 29, 1700924.
- [120] J. Li, J. Wu, H. Wang, Y. Lu, T. Ye, M. Sasase, X. Wu, M. Kitano, T. Inoshita, H. Hosono, *Chem. Sci.* **2019**, 10, 5712.
- [121] J. Wu, J. Li, Y. Gong, M. Kitano, T. Inoshita, H. Hosono, *Angew. Chem., Int. Ed.* **2019**, 58, 825.
- [122] S. Hagen, R. Barfod, R. Fehrmann, C. J. Jacobsen, H. T. Teunissen, K. Ståhl, I. Chorkendorff, *Chem. Commun.* **2002**, 1206.
- [123] W. Raróg-Pilecka, E. Miśkiewicz, M. Matyszek, Z. Kaszukur, L. Kępiński, Z. Kowalczyk, *J. Catal.* **2006**, 237, 207.
- [124] W. Raróg-Pilecka, E. Miśkiewicz, L. Kępiński, Z. Kaszukur, K. Kielar, Z. Kowalczyk, *J. Catal.* **2007**, 249, 24.
- [125] W. Raróg-Pilecka, E. Miśkiewicz, Z. Kowalczyk, *Catal. Commun.* **2008**, 9, 870.
- [126] W. Raróg-Pilecka, M. Karolewska, E. Truszkiewicz, E. Iwanek, B. Mierzwa, *Catal. Lett.* **2011**, 141, 678.
- [127] M. Karolewska, E. Truszkiewicz, B. Mierzwa, L. Kępiński, W. Raróg-Pilecka, *Appl. Catal., A* **2012**, 445–446, 280.
- [128] M. Karolewska, E. Truszkiewicz, M. Wściseł, B. Mierzwa, L. Kępiński, W. Raróg-Pilecka, *J. Catal.* **2013**, 303, 130.
- [129] B. Lin, Y. Qi, K. Wei, J. Lin, *RSC Adv.* **2014**, 4, 38093.
- [130] L. Zhang, J. Lin, J. Ni, R. Wang, K. Wei, *Catal. Commun.* **2011**, 15, 23.
- [131] A. Tarka, M. Zybert, E. Truszkiewicz, B. Mierzwa, L. Kępiński, D. Moszyński, W. Raróg-Pilecka, *ChemCatChem* **2015**, 7, 2836.
- [132] K. McAulay, J. S. J. Hargreaves, A. R. McFarlane, D. J. Price, N. A. Spencer, N. Bion, F. Can, M. Richard, H. F. Greer, W. Z. Zhou, *Catal. Commun.* **2015**, 68, 53.
- [133] M. Zybert, M. Karasińska, E. Truszkiewicz, B. Mierzwa, W. Raróg-Pilecka, *Polish J. Chem. Technol.* **2015**, 17, 138.
- [134] T. N. Ye, S. W. Park, Y. Lu, J. Li, M. Sasase, M. Kitano, T. Tada, H. Hosono, *Nature* **2020**, 583, 391.
- [135] R. Kojima, K.-I. Aika, *Appl. Catal., A* **2001**, 218, 121.
- [136] N. Bion, F. Can, J. Cook, J. S. J. Hargreaves, A. L. Hector, W. Levason, A. R. McFarlane, M. Richard, K. Sardar, *Appl. Catal., A* **2015**, 504, 44.
- [137] N. Segal, F. Sebba, *J. Catal.* **1967**, 8, 113.
- [138] G. I. Panov, A. S. Kharitonov, *React. Kinet. Catal. Lett.* **1985**, 29, 267.
- [139] D. A. King, F. Sebba, *J. Catal.* **1965**, 4, 253.
- [140] M. R. Hillis, C. Kemball, M. W. Roberts, *Trans. Faraday Soc.* **1966**, 62, 3570.
- [141] R. Kojima, K. Aika, *Appl. Catal., A* **2001**, 209, 317.
- [142] N. Segal, F. Sebba, *J. Catal.* **1967**, 8, 105.
- [143] J. S. J. Hargreaves, *Coord. Chem. Rev.* **2013**, 257, 2015.
- [144] C. J. Jacobsen, S. Dahl, B. S. Clausen, S. Bahn, A. Logadottir, J. K. Nørskov, *J. Am. Chem. Soc.* **2001**, 123, 8404.
- [145] C. J. H. Jacobsen, *Chem. Commun.* **2000**, 1057.
- [146] R. Kojima, K.-I. Aika, *Appl. Catal., A* **2001**, 215, 149.
- [147] R. Kojima, K.-I. Aika, *Appl. Catal., A* **2001**, 219, 157.
- [148] D. McKay, J. S. J. Hargreaves, J. L. Rico, J. L. Rivera, X. L. Sun, *J. Solid State Chem.* **2008**, 181, 325.
- [149] H. Cao, J. Guo, F. Chang, C. Pistidda, W. Zhou, X. Zhang, A. Santoru, H. Wu, N. Schell, R. Niewa, P. Chen, *Chem. Eur. J.* **2017**, 23, 9766.
- [150] T. N. Ye, S. W. Park, Y. Lu, J. Li, M. Sasase, M. Kitano, H. Hosono, *J. Am. Chem. Soc.* **2020**, 142, 14374.
- [151] S. Ghosh, S. M. Jeong, S. R. Polaki, *Korean J. Chem. Eng.* **2018**, 35, 1389.
- [152] G. S. Parkinson, *Surf. Sci. Rep.* **2016**, 71, 272.
- [153] P. Wang, H. Xie, J. Guo, Z. Zhao, X. Kong, W. Gao, F. Chang, T. He, G. Wu, M. Chen, L. Jiang, *Angew. Chem., Int. Ed.* **2017**, 56, 8716.
- [154] S. Hagen, R. Barfod, R. Fehrmann, C. J. Jacobsen, H. T. Teunissen, I. Chorkendorff, *J. Catal.* **2003**, 214, 327.
- [155] N. Morlanés, W. Almaksoud, R. K. Rai, S. Ould-Chikh, M. M. Ali, B. Vidjayacoumar, B. E. Al-Sabban, K. Albahily, J. M. Basset, *Catal. Sci. Technol.* **2020**, 10, 844.
- [156] P. Yan, W. Guo, Z. Liang, W. Meng, Z. Yin, S. Li, M. Li, M. Zhang, J. Yan, D. Xiao, R. Zou, *Nano Res.* **2019**, 12, 2341.
- [157] A. Jafari, A. Ebadi, S. Sahebdehfar, *React. Kinet. Mech. Catal.* **2019**, 126, 307.
- [158] W. Raróg-Pilecka, A. Jedynek-Koczuk, J. Petryk, E. Miśkiewicz, S. Jodzis, Z. Kaszukur, Z. Kowalczyk, *Appl. Catal., A* **2006**, 300, 181.
- [159] H. Fan, X. Huang, K. Kähler, J. Folke, F. Girgsdies, D. Teschner, Y. Ding, K. Hermann, R. Schlögl, E. Frei, *ACS Sustainable Chem. Eng.* **2017**, 5, 10900.
- [160] Ł. Czekajło, Z. Lendzion-Bieluń, *Catal. Today* **2017**, 286, 114.
- [161] H. B. Chen, J. D. Lin, Y. Cai, X. Y. Wang, J. Yi, J. Wang, G. Wei, Y. Z. Lin, D. W. Liao, *Appl. Surf. Sci.* **2001**, 180, 328.
- [162] J. Li, M. Kitano, T. N. Ye, M. Sasase, T. Yokoyama, H. Hosono, *ChemCatChem* **2017**, 9, 3078.
- [163] J. Z. Qiu, J. Hu, J. Lan, L. F. Wang, G. Fu, R. Xiao, B. Ge, J. Jiang, *Chem. Mater.* **2019**, 31, 9413.
- [164] N. Shimoda, Y. Kimura, Y. Kobayashi, J. Kubota, S. Satokawa, *Int. J. Hydrogen Energy* **2017**, 42, 29745.
- [165] J. Zhao, J. Zhou, M. Yuan, Z. You, *Catal. Lett.* **2017**, 147, 1363.
- [166] M. Chen, M. Yuan, J. Li, Z. You, *Appl. Catal., A* **2018**, 554, 1.
- [167] K. N. Iost, V. L. Temerev, N. S. Smirnova, D. A. Shlyapin, V. A. Borisov, I. V. Muromtsev, M. V. Trenikhin, T. V. Kireeva, A. V. Shilova, P. G. Tsyrl'nikov, *Russ. J. Appl. Chem.* **2017**, 90, 887.
- [168] M. Nishi, S.-Y. Chen, H. Takagi, *Catalysts* **2019**, 9, 406.
- [169] M. Nishi, S.-Y. Chen, H. Takagi, *ChemCatChem* **2018**, 10, 3411.
- [170] M. Nishi, S.-Y. Chen, H. Takagi, *Catalysts* **2019**, 9, 480.
- [171] K. Sato, K. Imamura, Y. Kawano, S. I. Miyahara, T. Yamamoto, S. Matsumura, K. Nagaoka, *Chem. Sci.* **2017**, 8, 674.
- [172] Y. Wu, C. Li, B. Fang, X. Wang, J. Ni, B. Lin, J. Lin, L. Jiang, *Chem. Commun.* **2020**, 56, 1141.
- [173] Z. Zhang, C. Karakaya, R. J. Kee, J. D. Way, C. A. Wolden, *ACS Sustainable Chem. Eng.* **2019**, 7, 18038.
- [174] B. Lin, L. Heng, H. Yin, B. Fang, J. Ni, X. Wang, J. Lin, L. Jiang, *Ind. Eng. Chem. Res.* **2019**, 58, 10285.
- [175] B. Lin, L. Heng, B. Fang, H. Yin, J. Ni, X. Wang, J. Lin, L. Jiang, *ACS Catal.* **2019**, 9, 1635.
- [176] Y. Ogura, K. Tsujimaru, K. Sato, S. I. Miyahara, T. Toriyama, T. Yamamoto, S. Matsumura, K. Nagaoka, *ACS Sustainable Chem. Eng.* **2018**, 6, 17258.

- [177] J. Li, W. Wang, W. Chen, Q. Gong, J. Luo, R. Lin, H. Xin, H. Zhang, D. Wang, Q. Peng, W. Zhu, *Nano Res.* **2018**, *11*, 4774.
- [178] Z. Ma, S. Zhao, X. Pei, X. Xiong, B. Hu, *Catal. Sci. Technol.* **2017**, *7*, 191.
- [179] R. Javaid, H. Matsumoto, T. Nanba, *ChemistrySelect* **2019**, *4*, 2218.
- [180] C. Liang, Z. Li, J. Qiu, C. Li, *J. Catal.* **2002**, *211*, 278.
- [181] Y. A. N. G. Xiaolong, X. I. A. Chungu, X. Xiong, M. U. Xinyuan, H. U. Bin, *Chin. J. Catal.* **2010**, *31*, 377.
- [182] K. Imamura, S. I. Miyahara, Y. Kawano, K. Sato, Y. Nakasaka, K. Nagaoka, *J. Taiwan Inst. Chem. Eng.* **2019**, *105*, 50.
- [183] J. Ni, B. Jing, J. Lin, B. Lin, Z. Zhao, L. Jiang, *J. Rare Earths* **2018**, *36*, 135.
- [184] W. Li, S. Wang, J. Li, *Chem. Asian J.* **2019**, *14*, 2815.
- [185] W. Li, P. Liu, R. Niu, J. Li, S. Wang, *Solid State Sci.* **2020**, *99*, 105983.
- [186] P. Liu, R. Niu, W. Li, S. Wang, J. Li, *Catal. Lett.* **2019**, *149*, 1007.
- [187] J. Zheng, F. Liao, S. Wu, G. Jones, T. Y. Chen, J. Fellowes, T. Sudmeier, I. J. McPherson, I. Wilkinson, S. C. E. Tsang, *Angew. Chem., Int. Ed.* **2019**, *58*, 17335.
- [188] P. Liu, R. Niu, W. Li, S. Wang, J. Li, *Energy Sources, Part A* **2019**, *41*, 689.
- [189] I. Luz, S. Parvathikar, M. Carpenter, T. Bellamy, K. Amato, J. Carpenter, M. Lail, *Catal. Sci. Technol.* **2020**, *10*, 105.
- [190] C. J. H. Jacobsen, *J. Catal.* **2001**, *200*, 1.
- [191] Y. Ma, G. Lan, X. Wang, G. Zhang, W. Han, H. Tang, H. Liu, Y. Li, *RSC Adv.* **2019**, *9*, 22045.
- [192] Y. Zhou, Y. Ma, G. Lan, H. Tang, W. Han, H. Liu, Y. Li, *Chin. J. Catal.* **2019**, *40*, 114.
- [193] W. Han, Z. Li, H. Liu, *J. Rare Earths* **2019**, *37*, 492.
- [194] Y. Ma, G. Lan, W. Fu, Y. Lai, W. Han, H. Tang, H. Liu, Y. Li, *J. Energy Chem.* **2020**, *41*, 79.
- [195] H. Abe, Y. Niwa, M. Kitano, Y. Inoue, M. Sasase, T. Nakao, T. Tada, T. Yokoyama, M. Hara, H. Hosono, *J. Phys. Chem. C* **2017**, *121*, 20900.
- [196] G. Hasegawa, S. Moriya, M. Inada, M. Kitano, M. Okunaka, T. Yamamoto, Y. Matsukawa, K. Nishimi, K. Shima, N. Enomoto, S. Matsuishi, *Chem. Mater.* **2018**, *30*, 4498.
- [197] Y. Inoue, M. Kitano, M. Tokunari, T. Taniguchi, K. Ooya, H. Abe, Y. Niwa, M. Sasase, M. Hara, H. Hosono, *ACS Catal.* **2019**, *9*, 1670.
- [198] I. AlShibane, A. Daisley, J. S. Hargreaves, A. L. Hector, S. Laassiri, J. L. Rico, R. I. Smith, *ACS Sustainable Chem. Eng.* **2017**, *5*, 9214.
- [199] W. Gao, P. Wang, J. Guo, F. Chang, T. He, Q. Wang, G. Wu, P. Chen, *ACS Catal.* **2017**, *7*, 3654.
- [200] X. Wang, X. Peng, W. Chen, G. Liu, A. Zheng, L. Zheng, J. Ni, C. T. Au, L. Jiang, *Nat. Commun.* **2020**, *11*, 653.
- [201] X. Wang, L. Li, T. Zhang, B. Lin, J. Ni, C. T. Au, L. Jiang, *Chem. Commun.* **2019**, *55*, 474.
- [202] R. Kojima, K.-I. Aika, *Chem. Lett.* **2000**, *29*, 912.
- [203] M. Zybert, M. Wyszynska, A. Tarka, W. Patkowski, H. Ronduda, B. Mierzwa, L. Kępiński, A. Sarnecki, D. Moszyński, W. Raróg-Pilecka, *Vacuum* **2019**, *168*, 108831.
- [204] H. Ronduda, M. Zybert, W. Patkowski, A. Tarka, P. Jodłowski, L. Kępiński, A. Sarnecki, D. Moszyński, W. Raróg-Pilecka, *Appl. Catal., A* **2020**, *598*, 117553.
- [205] B. Lin, Y. Liu, L. Heng, J. Ni, J. Lin, L. Jiang, *J. Rare Earths* **2018**, *36*, 703.
- [206] B. Lin, Y. Liu, L. Heng, J. Ni, J. Lin, L. Jiang, *Catal. Commun.* **2017**, *101*, 15.
- [207] S. Al Sobhi, N. Bion, J. S. Hargreaves, A. L. Hector, S. Laassiri, W. Levason, A. W. Lodge, A. R. McFarlane, C. Ritter, *Mater. Res. Bull.* **2019**, *118*, 110519.
- [208] S. Al Sobhi, J. S. Hargreaves, A. L. Hector, S. Laassiri, *Dalton Trans.* **2019**, *48*, 16786.



**John Humphreys** received his Ph.D. from the University of Warwick in 2019 on the topic of developing oxygen and steam-tolerant catalysts for ammonia synthesis. His research interests include the design of highly active catalysts that can operate at reduced temperature and pressure with a high tolerance to feed gas impurities.



**Shanwen Tao** is Professor of Chemical Engineering & Sustainable Processes in the School of Engineering, University of Warwick. His research interests include new ionic/electronic conducting materials for electrochemical devices such as fuel cells, electrolyzers, batteries, and supercapacitors. He is also interested in new catalysts for synthesis of ammonia and wastewater treatment through electrochemical processes.